from American Type Culture Collection (ATCC). In contrast, EhRab7D and 7G were poorly transcribed in an independently established attenuated HM-1 strain (Mitra et al., 2006; Saito-Nakano et al., 2007). These data suggest that the expression of individual Rab7 isotypes may be largely affected by subtle changes in the *in vitro* culture conditions.

3.2.4. Regulation of Rab gene expression during stage conversion

Several EhRab genes have been suggested to play a role in the stage conversion of *E. histolytica* (Ehrenkaufer et al., 2007). Transcriptomic analysis of clinical isolates and an attenuated HM-1 strain showed that EhRabM1 and EhRabN1 were expressed 6.7- and 4.1-fold higher in clinical isolates, respectively, than in HM-1 (Table 3). Since the clinical isolates used partially retained an ability to encyst *in vitro*, which attenuated HM-1 strain had lost, these data may indicate that the aforementioned Rabs are likely to be upregulated in the cyst or during encystation. In contrast, Rab5, 7D, 11A, 11B, 11D, B, C1, C5, C6, D2, H1, K2, M2, and X37, were expressed at higher levels in the laboratory strain, which does not encyst, compared to the clinical isolates, suggesting that these Rabs may be upregulated in the trophozoite stage (Ehrenkaufer et al., 2007). EhRabM1 was upregulated in the cyst stage and by oxidative stress, which may suggest a common role of EhRabM1 in stress response and differentiation. It is worth examining whether these changes are found in the cyst-like form of *E. histolytica* induced by oxidative stress (Aguliar-Diaz et al., 2010).

In summary, we proposed the annotation of *E. invadens* and *E. histolytica* Rab genes. Comparison of the Rab repertoire between the two species demonstrated that the majority of Rabs is conserved between the two species, while there are also species-specific Rabs. To understand the individual roles of Rabs, further functional studies are necessary. For instance, comprehensive transcriptomic analysis of Rab genes during the encystation of *E. invadens* should identify stage-specific regulated Rab genes and reveal ubiquitous or species-specific Rab-mediated encystation mechanisms in *Entamoeba*.

Acknowledgments

We thank Lis Caler, Bioinformatics Resource Center, J. Craig Venter Institute for sharing unpublished information of the *E. invadens* genome, and Takashi Makiuchi for his help with the phylogenetic analyses. We thank Eiko Nakasone for her help in the search for Rab genes from *E. invadens*. This work was supported by Creative Scientific Research (18GS0314) from the Japanese Ministry of Education, Science, Culture, Sports, and Technology to T.N., a Grant-in-Aid for Scientific Research from the Japanese Ministry of Education, Culture, Sports, Science, and Technology to T.N. (18GS0314, 18050006, and 18073001), a grant for research on emerging and re-emerging infectious diseases from the Japanese Ministry of Health, Labour, and Welfare, and a grant for research to promote the development of anti-AIDS pharmaceuticals from the Japan Health Sciences Foundation to T.N.

References

Aguliar-Diaz, H., Diaz-Gallardo, M., Laclette, J.P., Carrero, C.J., 2010. In vitro induction of *Entamoeba histolytica* cyst-like structures from trophozoites. PLoS Neglected Tropical Diseases 4, e607.

Biller, L., Davis, P.H., Tillack, M., Matthiesen, J., Lotter, H., Stanley, S.L., Tannich, E., Bruchhaus, I., 2010. Differences in the transcriptome signatures of two genetically related *Entamoeba histolytica* cell lines derived from the same isolate with different pathogenic properties. BMC Genomics 11, 63.

Bourne, H.R., Sanders, D.A., McCormick, F., 1990. The GTPase superfamily: a conserved switch for diverse cell functions. Nature 348, 125–132.

Carlton, J.M., Hirt, R.P., Silva, J.C., Delcher, A.L., Schantz, M., Zhao, Q., Wortman, J.R., Bidwell, S.L., Alsmark, U.C., Besterio, S., Sicheritz-Ponten, T., Noel, C.J., Dacks, J.B., Foster, P.G., Simillion, C., et al., 2007. Draft genome sequence of the sexually transmitted pathogen *Trichomonas vaginalis*. Science 315, 207–212.

Chatterjee, A., Ghosh, S.K., Jang, K., Bullitt, E., Moore, L., Robbins, P.W., Samuelson, J., 2009. Evidence for a "wattle and daub" model of the cyst wall of *Entamoeba*. PLoS Pathogens 5, e1000498.

Ehrenkaufer, G.M., Haque, R., Hackney, J.A., Eichinger, D.J., Singh, U., 2007. Identification of developmentally regulated genes in *Entamoeba histolytica*: insights into mechanisms of stage conversion in a protozoan parasite. Cellular Microbiology 9, 1426–1444.

Eichinger, D., 1997. Encystation of *Entamoeba* parasites. Bioessays 19, 633–639.

Eichinger, D., 2001. Encystation in parasitic protozoa. Current Opinion in Microbiology 4, 421–426.

Gilchrist, C.A., Houpt, E., Trapaidze, N., Fei, Z., Crasta, O., Asgharpour, A., Evans, C., Martino-Catt, S., Baba, D.J., Stroup, S., Hamano, S., Ehrenkaufer, G., Okada, M., Singh, U., Nozaki, T., Mann, B.J., Petri Jr., W.A., 2006. Impact of intestinal colonization and invasion on the *Entamoeba histolytica* transcriptome. Molecular and Biochemical Parasitology 147, 163–176.

Juarez, P., Sanchez-Lopez, R., Stock, R.P., Olvera, A., Ramos, M.A., Alagon, A., 2001. Characterization of the EhRab8 gene, a marker of the late stages of the secretory pathway of *Entamoeba histolytica*. Molecular and Biochemical Parasitology 116, 223–228.

MacFarlane, R.C., Singh, U., 2006. Identification of differentially expressed genes in virulent and nonvirulent *Entamoeba* species: potential implications for amebic pathogenesis. Infection and Immunity 74, 340–351.

MacFarlane, R., Bhattacharya, D., Singh, U., 2005. Genomic DNA microarrays for *Entamoeba histolytica*: applications for use in expression profiling and strain genotyping. Experimental Parasitology 110, 196–202.

Marion, S., Laurent, C., Guillén, N., 2005. Signalization and cytoskeleton activity through myosin IB during the early steps of phagocytosis in *Entamoeba histolytica*: a proteomic approach. Cellular Microbiology 7, 1504–1518.

McGugan Jr., G.C., Temesvari, L.A., 2003. Characterization of a Rab11-like GTPase, EhRab11, of *Entamoeba histolytica*. Molecular and Biochemical Parasitology 129, 137–146.

Mitra, B.N., Yasuda, T., Kobayashi, S., Saito-Nakano, Y., Nozaki, T., 2005. Differences in morphology of phagosomes and kinetics of acidification and degradation in phagosomes between the pathogenic *Entamoeba histolytica* and the non-pathogenic *Entamoeba dispar*. Cell Motility and Cytoskeleton 62, 84–99.

Mitra, B.N., Kobayashi, S., Saito-Nakano, Y., Nozaki, T., 2006. *Entamoeba histolytica*: differences in phagosome acidification and degradation between attenuated and virulent strains. Experimental Parasitology 114, 57–61.

Mitra, B.N., Saito-Nakano, Y., Nakada-Tsukui, K., Sato, D., Nozaki, T., 2007. Rab11B small GTPase regulates secretion of cysteine proteases in the enteric protozoan parasite *Entamoeba histolytica*. Cellular Microbiology 9, 2112–2125.

Nakada-Tsukui, K., Saito-Nakano, Y., Ali, V., Nozaki, T., 2005. A retromerlike complex is a novel Rab7 effector that is involved in the transport of the virulence factor cysteine protease in the enteric protozoan parasite *Entamoeba histolytica*. Molecular Biology of the Cell 16, 5294–5303.

Novick, P., Zerial, M., 1997. The diversity of Rab proteins in vesicle transport. Current Opinion in Cell Biology 9, 496–504.

Nozaki, T., Nakada-Tsukui, K., 2006. Membrane trafficking as a virulence mechanism of the enteric protozoan parasite *Entamoeba histolytica*. Parasitology Research 98, 179–183.

Okada, M., Huston, C.D., Mann, B.J., Petri Jr., W.A., Kita, K., Nozaki, T., 2005. Proteomic analysis of phagocytosis in the enteric protozoan parasite *Entamoeba histolytica*. Eukaryotic Cell 4, 827–831.

Okada, M., Huston, C.D., Oue, M., Mann, B.J., Petri Jr., W.A., Kita, K., Nozaki, T., 2006. Kinetics and strain variation of phagosome proteins of *Entamoeba histolytica* by proteomic analysis. Molecular and Biochemical Parasitology 145, 171–183.

Pereira-Leal, J.B., Seabra, M.C., 2000. The mammalian Rab family of small GTPases: definition of family and subfamily sequence motifs suggests a mechanism for functional specificity in the Ras superfamily. Journal of Molecular Biology 301, 1077–1087.

Pereira-Leal, J.B., Seabra, M.C., 2001. Evolution of the Rab family of small GTP-binding proteins. Journal of Molecular Biology 313, 889–901.

Picazarri, K., Nakada-Tsukui, K., Nozaki, T., 2008. Autophagy during proliferation and encystation in the protozoan parasite *Entamoeba invadens*. Infection and Immunity 76, 278–288.

Rodriguez, M.A., Garcia-Perez, R.M., Garcia-Rivera, G., Lopez-Reyes, I., Mendoza, L., Ortiz-Navarrete, V., Orozco, E., 2000. An *Entamoeba histolytica* rab-like encoding gene and protein: function and cellular location. Molecular and Biochemical Parasitology 108, 199–206.

Romero-Diaz, M., Gomez, C., Lopez-Reyes, I., Martinez, M.B., Orozco, E., Rodriguez, M.A., 2007. Structural and functional analysis of the *Entamoeba histolytica* EhrabB gene promoter. BMC Molecular Biology 8, 82.

Saito-Nakano, Y., Yasuda, T., Nakada-Tsukui, K., Leippe, M., Nozaki, T., 2004. Rab5-associated vacuoles play a unique role in phagocytosis of the enteric protozoan parasite *Entamoeba histolytica*. Journal of Biological Chemistry 279, 49497–49507.

Saito-Nakano, Y., Loftus, B.J., Hall, N., Nozaki, T., 2005. The diversity of Rab GTPases in *Entamoeba histolytica*. Experimental Parasitology 110, 244–252.

Saito-Nakano, Y., Mitra, B.N., Nakada-Tsukui, K., Sato, D., Nozaki, T., 2007. Two Rab7 isotypes, EhRab7A and EhRab7B, play distinct roles in biogenesis of lysosomes and phagosomes in the enteric protozoan parasite *Entamoeba histolytica*. Cellular Microbiology 9, 1796–1808.

Saitou, N., Nei, M., 1987. The neighbor-joining method: a new method for reconstructing phylogenetic trees. Molecular Biology of Evolution 4, 406–425.

Singh, U., Ehrenkaufer, G.M., 2009. Recent insights into *Entamoeba* development: identification of transcriptional networks associated with stage conversion. International Journal of Parasitology 39, 41–47.

Stenmark, H., 2009. Rab GTPases as coordinators of vesicle traffic. Nature Reviews Molecular Cell Biology 10, 513–525.

Takai, Y., Sasaki, T., Matozaki, T., 2001. Small GTP-binding proteins. Physiological Reviews 81, 153–208.

Temesvari, L.A., Harris, E.N., Stanely, S.L., Cardelli, J.A., 1999. Early and late endosomal compartments of *Entamoeba histolytica* are enriched in cysteine proteases, acid phosphatase and several Ras-related Rab GTPases. Molecular and Biochemical Parasitology 103, 225–241.

Thompson, D.J., Higgins, D.G., Gibson, T.J., 1994. CLUSTAL W: improving the sensitivity of program multiple sequence alignment through sequence weighting, positive-specific gap penalties and weight matrix choice. Nucleic Acids Research 22, 4673–4680.

Vicente, J.B., Ehrenkaufer, G.M., Saraiva, L.M., Teixeira, M., Singh, U., 2009. *Entamoeba histolytica* modulates a complex repertoire of novel genes in response to oxidative and nitrosative stresses: implications for amebic pathogenesis. Cellular Microbiology 11, 51–69.

Wang, Z., Samuelson, J., Clark, C.G., Eichinger, D., Paul, J., Van Dellen, K., Hall, N., Anderson, I., Loftus, B., 2003. Gene discovery in the *Entamoeba invadens* genome. Molecular and Biochemical Parasitology 129, 23–31.

Welter, B.H., Temesvari, L.A., 2004. A unique Rab GTPase, EhRabA, of *Entamoeba histolytica*, localizes to the leading edge of motile cells. Molecular and Biochemical Parasitology 135, 185–195.

Welter, B.H., Temesvari, L.A., 2009. Overexpression of a mutant form of EhRabA, a unique Rab GTPase of *Entamoeba histolytica*, alters endoplasmic reticulum morphology and localization of the Gal/GalNAc adherence lectin. Eukaryotic Cell 8, 1014–1026.

Welter, B.H., Powell, R.R., Leo, M., Smith, C.M., Temesvari, L.A., 2005. A unique Rab GTPase, EhRabA, is involved in motility and polarization of *Entamoeba histolytica* cells. Molecular and Biochemical Parasitology 140, 161–173.

J. Eukaryot. Microbiol., ■(■), 2010 pp. 1–11

DOI: 10.1111/j.1550-7408.2010.00503.x

Marked Amplification and Diversification of Products of *ras* Genes from Rat Brain, Rab GTPases, in the Ciliates *Tetrahymena thermophila* and *Paramecium tetraurelia*

YUMIKO SAITO-NAKANO,[a,1] TOHRU NAKAHARA,[b,1] KENTARO NAKANO,[b] TOMOYOSHI NOZAKI[a] and OSAMU NUMATA[b]

[a]*Department of Parasitology, National Institute of Infectious Diseases, 1-23-1 Toyama, Shinjuku-ku, Tokyo 162-8640, Japan, and*
[b]*Department of Structural Biosciences, Graduate School of Life and Environmental Sciences, University of Tsukuba, 1-1-1 Tennohdai, Tsukuba, Ibaraki 305-8577, Japan*

ABSTRACT. Small GTPase Rab (products of *ras* genes from rat brain) is a widely conserved molecular switch among eukaryotes and regulates membrane trafficking pathways. It is generally considered that the number of Rab encoded in the genome correlates with multicellularity; however, we found that unicellular ciliates *Tetrahymena thermophila* (*Tt*) and *Paramecium tetraurelia* (*Pt*) possess many more Rab genes in their genome than the 64 *Hs*Rab genes in the human genome. We succeeded in isolating 86 cDNA clones of 88 *Tt*Rab genes in the *Tetrahymena* genome. By comparing the amino acid sequence of Rab in humans and the budding yeast *Saccharomyces cerevisiae*, 42 *Tt*Rab belonged to subfamilies functionally characterized and designated as conventional Rab, while the remaining 44 *Tt*Rab were considered to be species-specific. To examine the diversity of Rab in ciliates, we searched for Rab genes in the genome database of *P. tetraurelia*. Overall, 229 *Pt*Rab genes were found and categorized as 157 conventional and 72 species-specific *Pt*Rab, respectively. Among them, nine *Pt*Rab genes showed high homology to seven *Tt*Rab, suggesting the conservation of ciliate-specific Rab. These data suggested that the range of Rab is markedly amplified and diversified in ciliates, which may support the elaborate cellular structures and vigorous phagocytosis of those organisms.

Key Words. Evolution, gene diversity, membrane traffic, phagocytosis, vesicular fusion.

IN intracellular membrane traffic accompanied with small vesicles budded from the donor membrane to target the acceptor membrane, small GTPase Rab (products of *ras* genes from rat brain) regulates membrane fusion in the appropriate organelles (Novick and Zerial 1997; Stenmark 2009). In general, the complexity and diversity of Rab genes correlate with the multicellularity of organisms: for example, unicellular yeast *Saccharomyces cerevisiae*, a nematode *Caenorhabditis elegans*, and human *Homo sapiens*, which consist of one, $\sim 10^3$, or 10^{13} cells, have 11, 29, and more than 60 Rab genes, respectively (Pereira-Leal and Seabra 2001). In multicellular organisms, Rab proteins can be expressed in a tissue-, organ-, or developmental stage-specific fashion (Seabra, Mules, and Hume 2002; Zerial and McBride 2001).

The GTPase cycle of Rab between GTP-bound active and GDP-bound inactive forms is important for membrane fusion (Takai, Sasaki, and Matozaki 2001). The inactive form of Rab is activated by guanine nucleotide exchange factor, and then GTP-bound active Rab participates in membrane fusion between a donor and target membrane. After the completion of membrane fusion, internal GTPase activity is accelerated by GTPase-activating protein.

According to the classification of Rab in *S. cerevisiae* and *H. sapiens*, Rab was divided into several subfamilies based on the amino acid sequences around Switch I and II sequences, which specified their subcellular localization and were important for the interaction with effecter molecules. For example, Rab5 and Rab7 regulate endocytosis on early and late endosomes, respectively (Bucci et al. 1992), Rab4 and Rab11 are involved in recycling from early endosomes (Ullrich et al. 1996; van der Sluijs et al. 1992), Rab1 fuses ER vesicles to the Golgi (Nuoffer et al. 1994), Rab6 localizes the Golgi cisternae (White et al. 1999), Rab8 regulates polarized secretion in the trans-Golgi network (Huber et al. 1993), and Rab2 is involved in membrane recycling toward ER (Tisdale 1999).

[1]Contributed equally.

Corresponding Author: O. Numata, Department of Structural Biosciences, Graduate School of Life and Environmental Sciences, University of Tsukuba, 1-1-1 Tennohdai, Tsukuba, Ibaraki 305-8577, Japan—Telephone number/FAX number: +81 29 853 6614; e-mail: numata@sakura.cc.tsukuba.ac.jp

Ciliates are classified into Alveolata, which is evolutionally distant from *S. cerevisiae* and *H. sapiens*. Among them, *Tetrahymena thermophila* (*Tt*) and *Paramecium tetraurelia* (*Pt*) have been well studied from the physiological aspect of the microstructures of organelles and the cytoskeleton, the course of nutrient uptake and digestion, and ciliary movement (Nilsson 1979; Paulin 1996). These organisms show rapid formation of large phagosomes and maintain elaborated membranous structure, including the alveolar sacs underlying the plasma membrane, to endow a cell with strength, a contractile vacuole for osmotic regulation, and a cell surface covered by numerous cilia and supported by the infraciliature. Therefore, intracellular membrane traffic in ciliates is expected to be vigorous.

Supporting this assumption, 69 Rab genes were reported from the fully sequenced macronuclear genome in *T. thermophila* (Eisen et al. 2006). In addition, we further searched the genome database, and identified 19 additional *Tt*Rab genes. Among all 88 *Tt*Rab genes, the expression of 86 *Tt*Rab genes was confirmed from the proliferative stage of cells by isolating mRNA and synthesis of cDNA. In addition, a diversity of Rab genes was also observed in *P. tetraurelia*, suggesting that membrane traffic in ciliates may be highly developed.

MATERIALS AND METHODS

Isolation of Rab genes from macronuclear genome in *Tetrahymena thermophila*. *Tetrahymena thermophila* was previously reported to possess 69 Rab genes (Eisen et al. 2006). We searched for more Rab genes in the *T. thermophila* macronuclear genome database (Tetrahymena Genome Database Wiki; http://ciliate.org/index.php/home/welcome) and confirmed them by the presence of a conserved GTP-binding consensus domain (Box1: GDXXVGKT/S, Box2: DXXG, Box3: GNKXD, Box4: SXK) and a Rab family-specific sequence (RabF1: IGVDF, RabF2: KLQIW, RabF3: RFRSIT, RabF4: YYRGA, RabF5: LVYDIT) (Pereira-Leal and Seabra 2001).

cDNA cloning and sequence of *Tetrahymena thermophila* Rab genes. *Tetrahymena thermophila* CH1 strain was cultured in Neff medium (1% [w/v] Proteose Peptone No. 3 [Becton, Dickinson and Company, Franklin Lakes, NJ], 0.5% [w/v] yeast extract [Becton, Dickinson and Company], 0.87% [w/v] D-glucose, 33 μM $FeCl_2$) at 30 °C. cDNA was synthesized by the

SuperScript™ First-Strand Synthesis System (Life Technologies, Carlsbad, CA) using a random primer and total RNA purified from TRIzol (Life Technologies). All Rab genes were amplified from cDNA using each Rab-specific primer (supporting information Table S1). Amplified fragments were subjected to sequencing with an ABI Prism DNA sequencer 377 (Life Technologies).

Sequence alignment and phylogenetic analysis. The 86 deduced *Tt*Rab amino acid sequences stretching from the first to the third conserved GTP-binding consensus regions were aligned using the default parameters of the CLUSTAL W program version 1.83 (Thompson, Higgins, and Gibson 1994), together with six Rab proteins from *S. cerevisiae* and nine Rab proteins from human. Because of the unsuccessful cloning of cDNA corresponding to the N-terminal region of *Tt*Rab2D, the deduced amino acids used for phylogenetic analysis were retrieved from the TIGR database. After alignments were manually corrected and non-aligned gaps were removed using BioEdit software (http://www.mbio.ncsu.edu/bioedit/bioedit.html), unambiguously aligned sites were selected and used for phylogenetic analysis by the neighbor-joining method (Swofford et al. 2001) according to a pioneering study classifying the Rab GTPases in fungi and animals by Pereira-Leal and Seabra (2001). Phylogenetic trees were drawn using TreeView software (http://taxonomy.zoology.gla.ac.uk/rod/treeview.html). Bootstrap proportions (%) were obtained from 1,000 pseudoreplicate datasets. A *Tt*Rab showing >40% identity to human or yeast Rab was considered to be their homolog (i.e. a conventional Rab) while a *Tt*Rab showing <40% identity was considered to be a species-specific Rab (Pereira-Leal and Seabra 2001; Wilson, Kreychman, and Gerstein 2000).

Classification of *Paramecium tetraurelia* Rab. Genes encoding putative Rab were identified from the *Paramecium* database (http://paramecium.cgm.cnrs-gif.fr/db/index) using an approach similar to that for *Tt*Rab. As many Rab consisted of isoforms due to at least three whole genome duplications in *P. tetraurelia* (Aury et al. 2006), *Pt*Rab genes showing more than 85% identity were considered to be the same isoforms. One isoform was used for phylogenetic analysis.

RESULTS

Cloning of 86 *Tetrahymena thermophila* Rab genes. We manually checked the amino acid sequences conserved for Rab GTPase in 69 *Tt*Rab genes, and found two errors in the database (http://ciliate.org/index.php/home/welcome): an ORF named *Tt*Rab64 (TTHERM_00194460) encodes Ran GTPase-activating protein but not Rab GTPase; and an ORF named *Tt*Rab45 (TTHERM_00207260) showed the potential fusion of two genes encoding Rab individually, indicating an incorrect exon–intron prediction.

Following cDNA cloning, we confirmed expression of 86 *Tt*Rab genes from the vegetative growth stage. The *Tetrahymena* gene expression database (TGED; http://tg ed.ihb.ac.cn/) (Miao et al. 2009) supports this conclusion although several *rab* genes are markedly expressed during starvation or conjugation as compared with a logarithmic growing phase (Fig. S1 and S2, see below for details). Our cDNA cloning also revealed that one ORF, named *Tt*Rab45 (TTHERM_00207260), was transcribed independently of two Rab genes, RabX1A and RabX1E. On the other hand, we failed to amplify another two *Tt*Rab, TTHERM_00637520 and TTHERM_00985100, of which gene expression is low throughout every stages of a life cycle studied in TGED (Fig. S2F). It is unknown why those cDNA were not amplified nevertheless another cDNA, expressed lower than them, was identified in our experimental condition. In addition, cloning of the N-terminus region of *Tt*Rab2D was unsuccessful for unknown reason.

Classification of *Tetrahymena thermophila* Rab genes. Forty-two of 86 *Tt*Rab genes showed high identity (>40%) to human Rab1 (i.e. *S. cerevisiae* [*Sc*] Ypt1p), Rab2/Rab4, Rab5 (*Sc*Ypt51p), Rab6 (*Sc*Ypt6p), Rab7 (*Sc*Ypt7p), Rab8 (*Sc*Sec4p), and Rab11 (*Sc*Ypt31p). They were classified into conventional Rab and named *Tt*Rab1A–*Tt*Rab1F (six isotypes), *Tt*Rab8A–*Tt*Rab8G (seven isotypes), *Tt*Rab2A–*Tt*Rab2G (seven isotypes), *Tt*Rab4A and *Tt*Rab4B (two isotypes), *Tt*Rab11A–*Tt*Rab11I (nine isotypes), *Tt*Rab5A–*Tt*Rab5C (three isotypes), *Tt*Rab21A–*Tt*Rab21C (three isotypes), *Tt*Rab6A–*Tt*Rab6D (four isotypes), and *Tt*Rab7 (Fig. 1, Table 1, Tables S2–S8). The remaining 44 *Tt*Rab genes, which showed <40% identity to Rab from other organisms, were concluded to be species specific. Among then, 12 of 44 species-specific Rab were classified into three subfamilies, *Tt*RabX1A–*Tt*RabX1H (eight isotypes), *Tt*RabX2A and *Tt*RabX2B (two isotypes), and *Tt*RabX3A and *Tt*RabX3B (two isotypes), based on their >40% identity (Fig. 1, Table 1, Table S9). Another 32 *Tt*Rab did not show identity to any other Rab and were named *Tt*RabX4–*Tt*RabX35 (Fig. 1, Table 1).

Annotation of conventional *Tt*Rab genes. Rab5 localizes in early endosomes, and regulates fusion between early endosomes in the endocytic pathway in other organisms (Bucci et al. 1992; Horazdovsky, Busch, and Emr 1994; Singer-Kruger, Stenmark, and Zerial 1995). Human and *S. cerevisiae* possess three isotypes of Rab5 (Takai et al. 2001). In *T. thermophila*, three *Tt*Rab5 isotypes (*Tt*Rab5A–*Tt*Rab5C) were also present, one of which, *Tt*Rab5C, was annotated previously as species-specific *Tt*Rab (*Tt*Rab55) in the genome database, because of an error in the exon–intron prediction (Table S2). Our cloned cDNA sequence of *Tt*Rab55 showed 41% identity to *Tt*Rab5A, and was renamed *Tt*Rab5C. According to the information of TGED, all three *Tt*Rab5 isotypes seem to be constitutively expressed throughout a life cycle while expression level of *Tt*Rab5A and *Tt*Rab5B is much higher than *Tt*Rab5C (Fig. S1E).

Human Rab21, which is categorized into the Rab5 subfamily (Pereira-Leal and Seabra 2001), also localizes to endosomes and has a role in the endocytic pathway. Humans possess one Rab21 gene, which is not present in *S. cerevisiae* (Pereira-Leal and Seabra 2001). In *T. thermophila*, one of the three isotypes of *Tt*Rab21 (*Tt*Rab21A–*Tt*Rab21C), *Tt*Rab21A, was newly identified in this work (Table 1). *Tt*Rab21A showed the highest identity (44%) to *Hs*Rab21 among the *Tt*Rab21 subfamily (Table S2). Interestingly, expression of *Tt*Rab21A transiently increases in cells at the onset of starvation according to the information of TGED (Fig. S1E) (Miao et al. 2009).

Rab7 regulates endocytosis from early to late endosomes, and also traffic to lysosomes (Bucci et al. 2000; Feng, Press, and Wandinger-Ness 1995). Humans and *S. cerevisiae* possess one Rab7 gene, respectively. *Tetrahymena thermophila* also possesses a single Rab7, showing 56% and 51% identities to *Hs*Rab7 and *Sc*Ypt7p, respectively (Fig. 1, Table S3). *Tt*Rab7 seems to be constitutively expressed throughout a life cycle (Fig. S1F), and localizes to phagosomes by immunofluorescence staining (Nakano and Numata, unpubl. data).

Rab1 localizes mainly in the Golgi, and regulates vesicle fusion to the Golgi (Nuoffer et al. 1994). Humans and *S. cerevisiae* possesses two and one Rab1 genes, respectively. In contrast, *T. thermophila* possesses six isotypes (*Tt*Rab1A–*Tt*Rab1F) of *Tt*Rab1 (Fig. 1, Table S4), and two isotypes, *Tt*Rab1B and *Tt*Rab1D, were mis-annotated as species-specific *Tt*Rab61 and *Tt*Rab62, respectively, in a previous study (Eisen et al. 2006). Our cDNA cloning predicted the exact primary sequence of *Tt*Rab1B (i.e. *Tt*Rab61) and *Tt*Rab1D (i.e. *Tt*Rab62), and revealed that they showed 55% and 49% identities to *Hs*Rab1, respectively. Remarkably, expression of *Tt*Rab1F is about 10-fold increased under the starvation condition while other five isotypes show a constitutive-expression pattern (Fig. S1A).

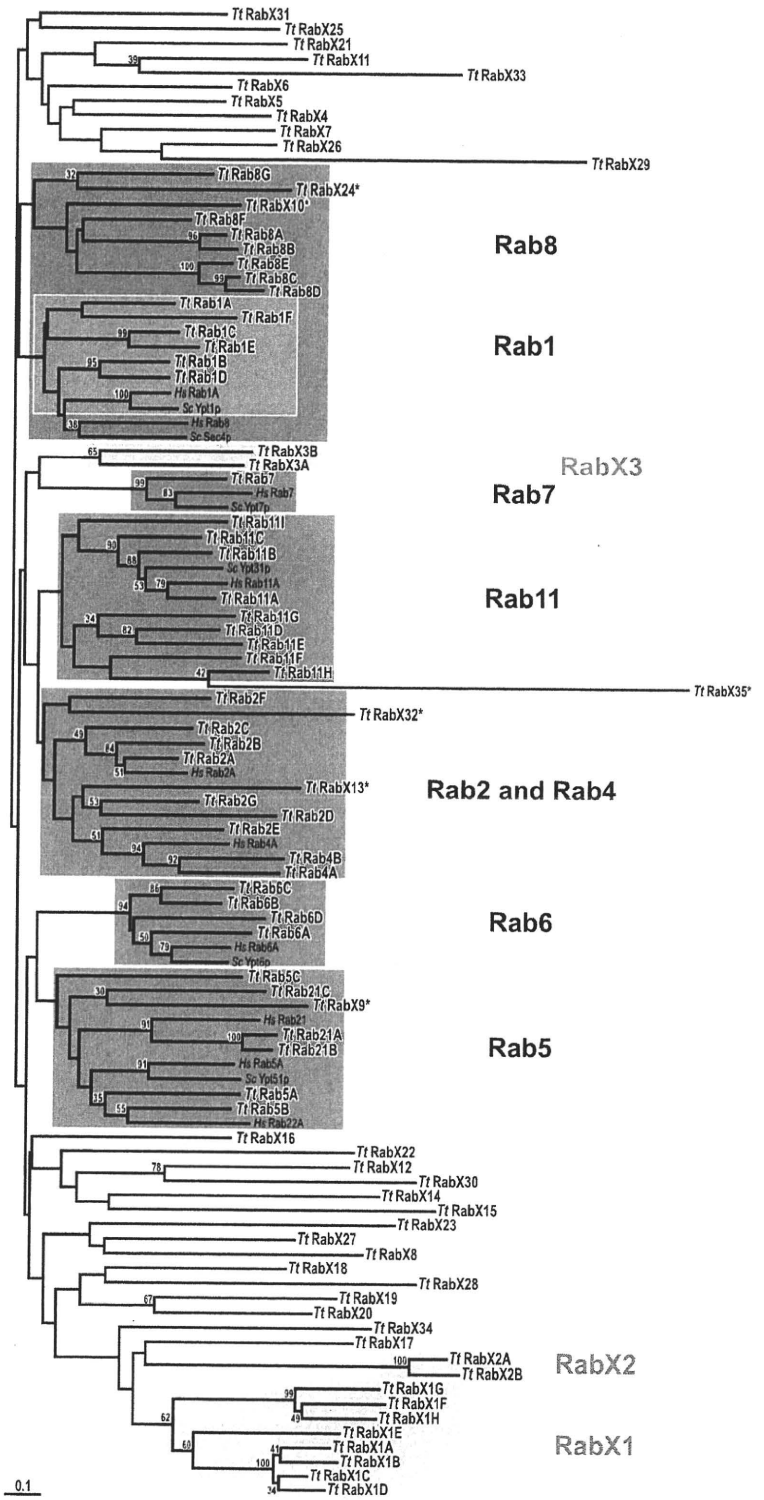

Fig. 1. A phylogenetic tree of gene products of *rab* (*ras* genes from rat brain) from *Tetrahymena thermophila*, *Homo sapiens*, and *Saccharomyces cerevisiae*. Bootstrap proportions >30% are shown. *Tetrahymena thermophila* Rab proteins are indicated in bold. Conventional Rab that revealed significant homology (>40% identity) to human or yeast counterparts are shaded by dark boxes, while three species-specific subfamilies are highlighted by light boxes. Asterisks indicate Rab proteins that were not considered as isotypes of the subfamily based on <40% identity to other isotypes. Scale bar indicates 0.1 substitutions at each amino acid position.

(BWUS JEU 503-4005 Webpdf: 08/05/2010 06:43:28 1456859 Bytes 11 PAGES : opera or : 18/5/2010 6:44:54 PM

Q5 Table 1. List of the Rab GTPases in *Tetrahymena thermophila*.

Subclass	Gene name proposed in this study	TGD annotation	Accession no. in TGD	Accession no. in DDBJ	Number of introns	Missing region	C-terminal prenylation motif	Length of amino acid residues
Conventional Rab								
Rab1	Rab1A	Rab1A	TTHERM_00316280	AB365891	1		XXCC	211
	Rab1B	Rab61	TTHERM_00784530	AB365895	6		XXCC	212
	Rab1C	Rab1C	TTHERM_00825210	AB365893	0		XXCC	210
	Rab1D	Rab62	TTHERM_01129680	AB365896	7		XXCC	223
	Rab1E	Rab1B	TTHERM_00433430	AB365892	0		CCXX	250
	Rab1F	Rab1D	TTHERM_00419740	AB365894	0		XXCC	211
Rab8	Rab8A	Rab8A	TTHERM_00279750	AB365919	0		XXCC	205
	Rab8B	Rab8B	TTHERM_00225720	AB365920	0		XXCC	204
	Rab8C	Rab64	TTHERM_00083660	AB365955	2		XXCC	204
	Rab8D	Rab65	TTHERM_00083670	AB365956	1		XXCC	204
	Rab8E	—	TTHERM_00083650	AB365974	1		XXCC	222
	Rab8F	Rab13A	TTHERM_00126950	AB365922	1		XXCC	207
	Rab8G	Rab60	TTHERM_00727540	AB365954	0		XCXC	250
Rab2 and Rab4	Rab2A	Rab2A	TTHERM_00467790	AB365897	5		XXCC	211
	Rab2B	Rab2B	TTHERM_00670290	AB365898	4		XXCC	218
	Rab2C	Rab2C	TTHERM_00726080	AB365899	6		XXCC	223
	Rab2D	Rab2E	TTHERM_00994150	—	6	Box1	—	
	Rab2E	Rab2D	TTHERM_00579220	AB365924	5		XCXC	234
	Rab2F	Rab2F	TTHERM_00557870	AB365925	4		XCXC	235
	Rab2G	—	TTHERM_00245180	AB365960	4		XXCC	207
	Rab4A	Rab4B	TTHERM_01097960	AB365901	3		XCXC	212
	Rab4B	Rab4A	TTHERM_00001080	AB365900	3		XCXC	212
Rab11	Rab11A	Rab11A	TTHERM_00316600	AB365902	2		XXCC	230
	Rab11B	Rab11B	TTHERM_00941540	AB365903	2		XXCC	214
	Rab11C	Rab11C	TTHERM_00347990	AB365904	8		XXCC	221
	Rab11D	Rab11E	TTHERM_00389960	AB365906	0		CXCX	363
	Rab11E	—	TTHERM_00149110	AB365905	5		XCXC	206
	Rab11F	—	TTHERM_00354630	AB365966	2		XXCC	234
	Rab11G	Rab11F	TTHERM_01099240	AB365907	0		XCXC	214
	Rab11H	—	TTHERM_01085570	AB365961	5		CCCX	218
	Rab11I	Rab11D	TTHERM_00471070	AB365926	1		XXCX	225
Rab5	Rab5A	Rab5A	TTHERM_00711980	AB365908	6		XCXC	199
	Rab5B	Rab22	TTHERM_00794230	AB365914	6		XCXC	197
	Rab5C	Rab55	TTHERM_00711970	AB365949	5		XXCC	194
	Rab21A	—	TTHERM_00540110	AB365913	4		XXCC	201
	Rab21B	Rab21A	TTHERM_00540100	AB365912	4		XXCC	207
	Rab21C	Rab5C	TTHERM_00614720	AB365910	3		—	205
Rab6	Rab6A	Rab6A	TTHERM_00467760	AB365915	4		XXCC	229
	Rab6B	Rab6C	TTHERM_00079900	AB365917	3		XXCC	227
	Rab6C	Rab6B	TTHERM_01079210	AB365916	4		XCXC	224
	Rab6D	Rab6D	TTHERM_01164180	AB365918	4		XXCC	265
Rab7	Rab7	Rab7	TTHERM_00470810	AB024707	5		XCXC	200
Species-specific Rab								
RabX1	RabX1A	Rab45	TTHERM_00207260	AB365939	1	Box2	—	173
	RabX1B	Rab46	TTHERM_00209270	AB365940	1	Box2	—	175
	RabX1C	Rab47	TTHERM_00207250	AB365941	1	Box2	—	175
	RabX1D	—	TTHERM_00207240	AB365969	1	Box2	—	173

Subclass	Gene name proposed in this study	TGD annotation	Accession no. in TGD	Accession no. in DDBJ	Number of introns	Broken region	C-terminal prenylation motif	Length of amino acid residues
	RabX1E	**Rab45**	**TTHERM_00207260**	**AB365938**	**1**	**Box2**	**—**	**176**
	RabX1F	**Rab48**	**TTHERM_00201680**	**AB365942**	**1**	**Box2**	**—**	**174**
	RabX1G	**Rab50**	**TTHERM_00201700**	**AB365944**	**1**	**Box2**	**—**	**174**
	RabX1H	**Rab49**	**TTHERM_00201690**	**AB365943**	**1**		**—**	**174**
RabX2	RabX2A	Rab42	TTHERM_01407960	AB365935	1	Box2	—	184
	RabX2B	Rab43	TTHERM_01407950	AB365936	1	Box2	—	184
RabX3	**RabX3A**	**Rab66**	**TTHERM_00338360**	**AB365957**	**5**		**XXCC**	**270**
	RabX3B	**—**	**TTHERM_00294940**	**AB365968**	**4**		**XXCC**	**212**
	RabX4	Rab37	TTHERM_00295030	AB365930	1		XCCX	215
	RabX5	Rab40	TTHERM_00066880	AB365933	1		XCCX	229
	RabX6	Rab58	TTHERM_01041920	AB365952	0		XXCC	222
	RabX7	Rab36	TTHERM_00723170	AB365929	1		XXCC	226
	RabX8	Rab28	TTHERM_01164080	AB365923	5	Box2	CXXX	218
	RabX9	Rab5B	TTHERM_00334520	AB365909	1		—	203
	RabX10	Rab3A	TTHERM_00149430	AB365921	2		CXCX	207
	RabX11	Rab17A	TTHERM_00957580	AB365911	1		—	198
	RabX12	Rab32	TTHERM_00852850	AB365927	0		XXCC	233
	RabX13	Rab11G	TTHERM_00994240	AB365928	2		—	212
	RabX14	Rab38	TTHERM_00723010	AB365931	1		CCXX	217
	RabX15	Rab39	TTHERM_00188280	AB365932	1		XCCX	227
	RabX16	Rab41	TTHERM_00664060	AB365934	0		XXCC	234
	RabX17	Rab44	TTHERM_00558520	AB365937	1	Box2	CXXX	194
	RabX18	Rab51	TTHERM_00671970	AB365945	0		XXCC	226
	RabX19	Rab52	TTHERM_00024230	AB365946	0		XXXC	211
	RabX20	Rab53	TTHERM_00431230	AB365947	0	Box2	XXCX	239
	RabX21	Rab54	TTHERM_01079300	AB365948	5		—	294
	RabX22	Rab56	TTHERM_00107200	AB365950	4		XCXC	189
	RabX23	Rab57	TTHERM_00298510	AB365951	4		—	171
	RabX24	Rab59	TTHERM_00727520	AB365953	0		—	189
	RabX25	Rab67	TTHERM_00059450	AB365958	5		CCXXX	227
	RabX26	Rab69	TTHERM_00290900	AB365959	4		XCXC	213
	RabX27	—	TTHERM_00780800	AB365962	0		—	181
	RabX28	—	TTHERM_00666200	AB365963	1		CXXX	209
	RabX29	—	TTHERM_00575490	AB365964	0	Box2	—	215
	RabX30	—	TTHERM_00313310	AB365965	1	RabF1	XXCC	225
	RabX31	—	TTHERM_00681770	AB365967	1		XCXC	250
	RabX32	—	TTHERM_01085550	AB365970	5		—	208
	RabX33	—	TTHERM_00497270	AB365971	7	Box2, RabF1	—	213
	RabX34	—	TTHERM_00320039	AB365972	1		—	171
	RabX35	—	TTHERM_00823440	AB365973	1		—	348

Rab8 regulates transport from the trans-Golgi network to the plasma membrane (Guo et al. 1999; Huber et al. 1993). Human and *S. cerevisiae* possesses two and one Rab8 genes, respectively. In *T. thermophila*, the Rab8 subfamily consisted of seven isotypes (*Tt*Rab8A–*Tt*Rab8G) (Table 1), two of which, *Tt*Rab8C and *Tt*Rab8D, were annotated previously as species-specific Rab64 and Rab65 in the database, respectively. However, we uncovered errors in the exon–intron prediction of Rab64 and Rab65, and we have renamed them *Tt*Rab8C and *Tt*Rab8D, respectively. *Tt*Rab8C and *Tt*Rab8D showed 43% and 41% identities to *Sc*Sec4p (Table S5). Rab60 has been renamed *Tt*Rab8G, because Rab60 showed 42% identity to *Tt*Rab8F. *Tt*Rab8E was newly identified by us and showed 41% identity to *Sc*Sec4p (Fig. 1, Table S5). According to the information of TGED, almost all members in *Tt*Rab8 subfamily are constitutively expressed in various levels, and only gene expression of *Tt*Rab8B is markedly elevated under the starvation condition (Fig. S1C).

*Hs*Rab2 and *Hs*Rab4 were classified into the same subfamily according to their sequence similarity (Pereira-Leal and Seabra 2001); however, the function and subcellular localization of Rab2 and Rab4 were different. *Hs*Rab2 regulated fusion with vesicles to ER (Tisdale 1999), and *Hs*Rab4 had a role in recycling from early endosomes to the plasma membrane (van der Sluijs et al. 1992). These Rab were present in humans (two *Hs*Rab2 and two *Hs*Rab4 genes) but not *S. cerevisiae*. In *T. thermophila*, seven *Tt*Rab2 (*Tt*Rab2A–*Tt*Rab2G) and two *Tt*Rab4 (*Tt*Rab4A and *Tt*Rab4B) isotypes were identified (Fig. 1, Table S6). After the erroneous prediction of the exon–intron in the *Tt*Rab2D had been corrected, *Tt*Rab2D showed 45% identity to *Hs*Rab2A and 53% identity to *Tt*Rab2A (Table S6). *Tt*Rab2G was newly characterized by us and showed 47% identity to *Hs*Rab2A. Expression level of *Tt*Rab2D, which is failed cloning of N-terminus region, is very low as compared with other members of *Tt*Rab2 subfamily (Fig. S1B).

*Hs*Rab6 localizes to the Golgi and regulates transport among the Golgi cisternae (Martinez et al. 1994; White et al. 1999). Humans and *S. cerevisiae* possess three and one Rab6 genes, respectively. In contrast, *T. thermophila* possesses four Rab6 isotypes, annotated as *Tt*Rab6A–*Tt*Rab6D (Fig. 1, Table S7). TGED shows a tendency that expression levels of all members in *Tt*Rab6 subfamily are decreased in early conjugation stage when meiosis progresses (Fig. S1F) (Miao et al. 2009).

Two isotypes of *Hs*Rab11 regulate the recycling pathway from recycling endosomes to the plasma membrane (Wang et al. 2000). In *S. cerevisiae*, *Sc*Ypt31p and *Sc*Ypt32p play redundant roles in controlling vesicle traffic from the trans-Golgi network to endosomes (Jedd, Mulholland, and Segev 1997; Ullrich et al. 1996). Nine members of *Tt*Rab11, annotated as *Tt*Rab11A–*Tt*Rab11I, were significantly divergent (Fig. 1, Table S8). Among them, *Tt*Rab11E, *Tt*Rab11F, and *Tt*Rab11H were newly characterized by us, showing 42% identity to *Hs*Rab11A, 42% identity to *Sc*Ypt31p, and 40% identity to *Tt*Rab11F, respectively (Table S8). Interestingly, by searching a gene expression profile of *Tt*Rab11 isotypes in TGED we found drastic changes of their expression dependent on the life cycle: four members, *Tt*Rab11A, *Tt*Rab11C, *Tt*Rab11D, and *Tt*Rab11F, are up-regulated in early conjugation stage, while two members, *Tt*Rab11B and *Tt*Rab11I, are down-regulated (Fig. S1D). Moreover, gene-expression pattern of *Tt*Rab11G exhibits two peaks at the late logarithmic stage and the onset of conjugation, respectively (Fig. S1D).

Annotation of species-specific *Tt*Rab of *Tetrahymena thermophila*. Among 44 species-specific *Tt*Rab, 12 formed three subfamilies based on their >40% identity (Table 1). In the *Tt*RabX1 subfamily (i.e. *Tt*RabX1A–*Tt*RabX1H), *Tt*RabX1A and *Tt*RabX1E were found from *Tt*Rab45 (TTHERM_00207260), as described above, and *Tt*RabX1D was newly characterized by us. The *Tt*RabX1 subfamily had a common feature in that it was lacking C-terminal cysteine residues and one GTP-binding consensus Box2 (Table 1). The *Tt*RabX2 subfamily (i.e. *Tt*RabX2A, *Tt*RabX2B) also showed the same characteristics: loss of C-terminus cysteine residues and the Box2 domain. *Tt*RabX3B (i.e. *Tt*RabX3A, *Tt*RabX3B) was newly identified by us, and showed 41% amino acid identity to *Tt*RabX3A. The 32 remaining *Tt*Rab genes, which showed low identities to other Rab, were named *Tt*RabX4–*Tt*RabX35 (Table 1). Nine of them, *Tt*RabX27–*Tt*RabX35, were newly characterized by us. By searching TGED, several species-specific *Tt*Rab show a remarkable change of gene-expression pattern through the life cycle: gene expression of *Tt*RabX1C, *Tt*RabX7, *Tt*RabX22, and *Tt*RabX27, transiently increases at the early conjugation stage when meiosis progresses, *Tt*RabX15 and *Tt*RabX35 increase during fertilization, and *Tt*RabX17 and *Tt*RabX19 show two peaks in their expression in starvation and exconjugation (Fig. S2) (Miao et al. 2009).

Classification of 229 Rab in another ciliate *Paramecium tetraurelia*. To examine whether the diversity of Rab genes is specific to *T. thermophila*, Rab genes from another ciliate were identified and classified. *Paramecium tetraurelia* is a well-known ciliate whose genome sequence is fully available (Aury et al. 2006). We searched the database of the macronuclear genome of *P. tetraurelia*, and found 229 *Pt*Rab genes based on >40% amino acid identity to Rab from other organisms. The 229 *Pt*Rab were grouped into 157 conventional *Pt*Rab and 72 species-specific *Pt*Rab (Table S10). Among conventional *Pt*Rab, 157 *Pt*Rab were further classified into eight subfamilies, 57 genes in *Pt*Rab1 and *Pt*Rab8 subfamilies, 56 genes in *Pt*Rab2 and *Pt*Rab4 subfamilies, 23 genes in *Pt*Rab11 subfamily, eight genes in *Pt*Rab5 subfamily, 10 genes in *Pt*Rab6 subfamily, and three genes in *Pt*Rab7 subfamily (Fig. 2, Tables S10–S16). Because homologs of *Pt*Rab1 and *Pt*Rab8 were richer in diversity than human homologs, it was impossible to clearly separate *Pt*Rab1 and *Pt*Rab8, respectively; therefore, they were combined as *Pt*Rab1 and *Pt*Rab8 subfamilies (Fig. 2, Table S13). Four *Pt*Rab genes in 72 species-specific *Pt*Rab could be classified into a species-specific single subfamily (Table S17).

Seventeen percent of *Pt*Rab had a substitution or deletion of amino acid residue(s) in one of the GTP-binding consensus regions. Similar to the observation from *Tt*Rab, 92% of conventional *Pt*Rab possessed C-terminus cysteines whereas 57% species-specific *Pt*Rab carried the C-terminus cysteine residues. Some *Pt*Rab have three cysteine residues (i.e. CXCXC, CXCC, and CCCXXX), which has not been reported in other organisms (Table S10).

Ciliate-specific Rab conserved between *Tetrahymena thermophila* and *Paramecium tetraurelia*. Seven species-specific *Tt*Rab also showed high homology to some of the nine *Pt*Rab (Fig. 3, Table S18). These ciliate-specific Rab were grouped into seven subfamilies. First, *Tt*RabX6 showed 41% amino acid identity to *Pt*Rab_A47, which was categorized into the same subfamily as *Pt*Rab_C67, showing 67% identity to *Pt*Rab_A47. Second, *Tt*RabX9 showed 48% identity to *Pt*Rab_A54. Third, *Tt*RabX12 showed 47% identity to GSPATP00019429001. Fourth, *Tt*RabX23 showed 46% identity to GSPATP00013049001. Fifth, *Tt*RabX27 showed 47% identity to *Pt*Rab_C95, which showed 68% identity to GSPATP00018487001. Sixth, *Tt*RabX32 showed 66% identity to *Pt*Rab_A50. Seventh, *Tt*RabX33 showed 72% identity to GSPATP00034817001 (Table S18).

DISCUSSION

Amplification of conventional Rab in ciliates. We identified and classified a large number of *Tt*Rab into seven subfamilies of conventional *Tt*Rab (i.e. Rab1, Rab2 and Rab4, Rab5, Rab6, Rab7, Rab8, Rab11), and species-specific *Tt*Rab. Conventional

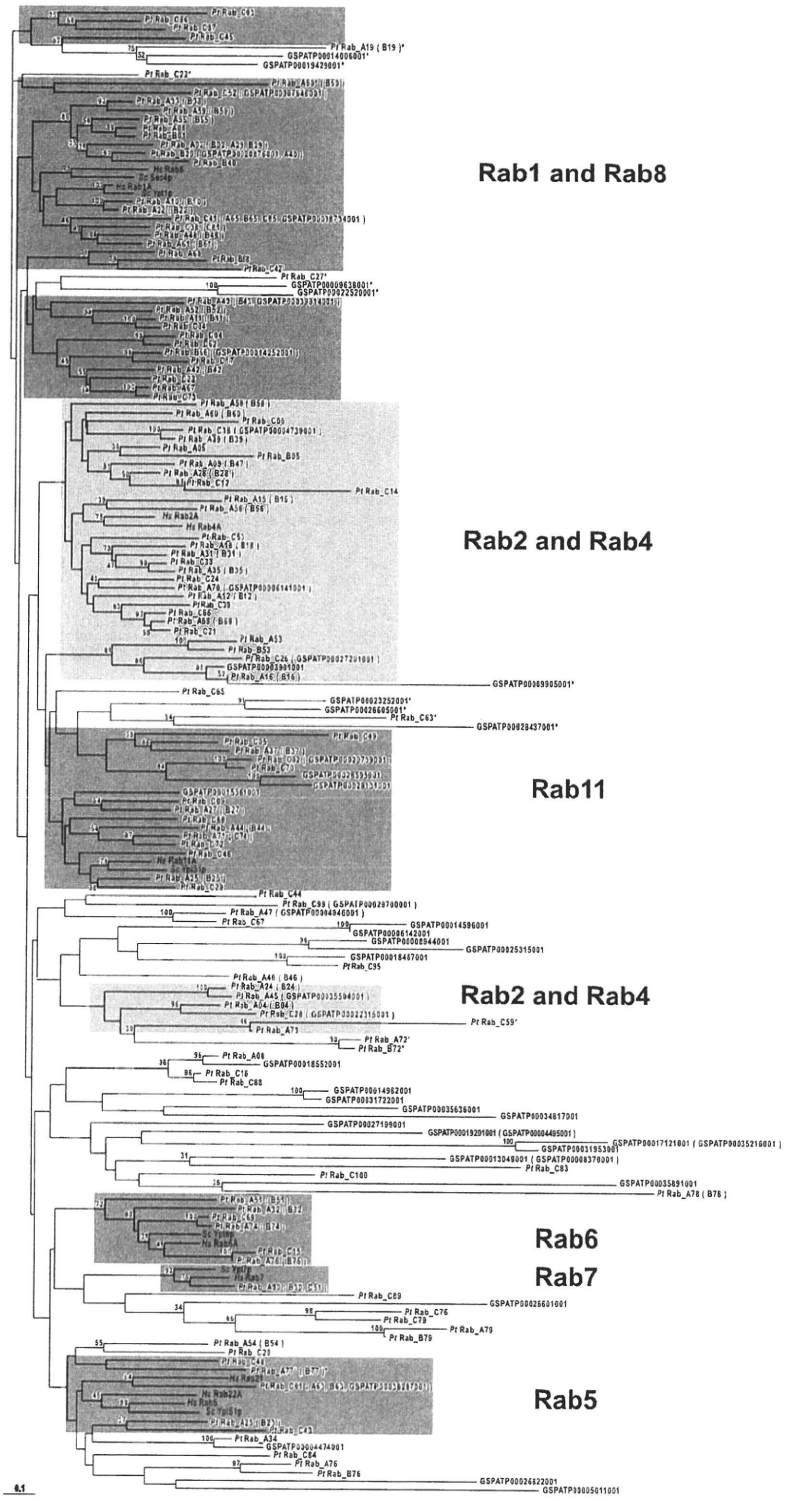

Fig. 2. A phylogenetic tree of gene products of *rab* (*ras* genes from rat brain) from *Paramecium tetraurelia*, *Homo sapiens*, and *Saccharomyces cerevisiae*. Bootstrap proportions >30% are shown. *Paramecium tetraurelia* Rab proteins are indicated in bold. *Pt*Rab isotypes arising from genome duplication are shown in parentheses. Conventional Rab that revealed significant homology (>40% identity) to human or yeast counterparts are shaded by dark- or light-boxes. Asterisks indicate Rab proteins that are not considered as isotypes of the subfamily based on <40% identity to other isotypes. Scale bar indicates 0.1 substitutions at each amino acid position.

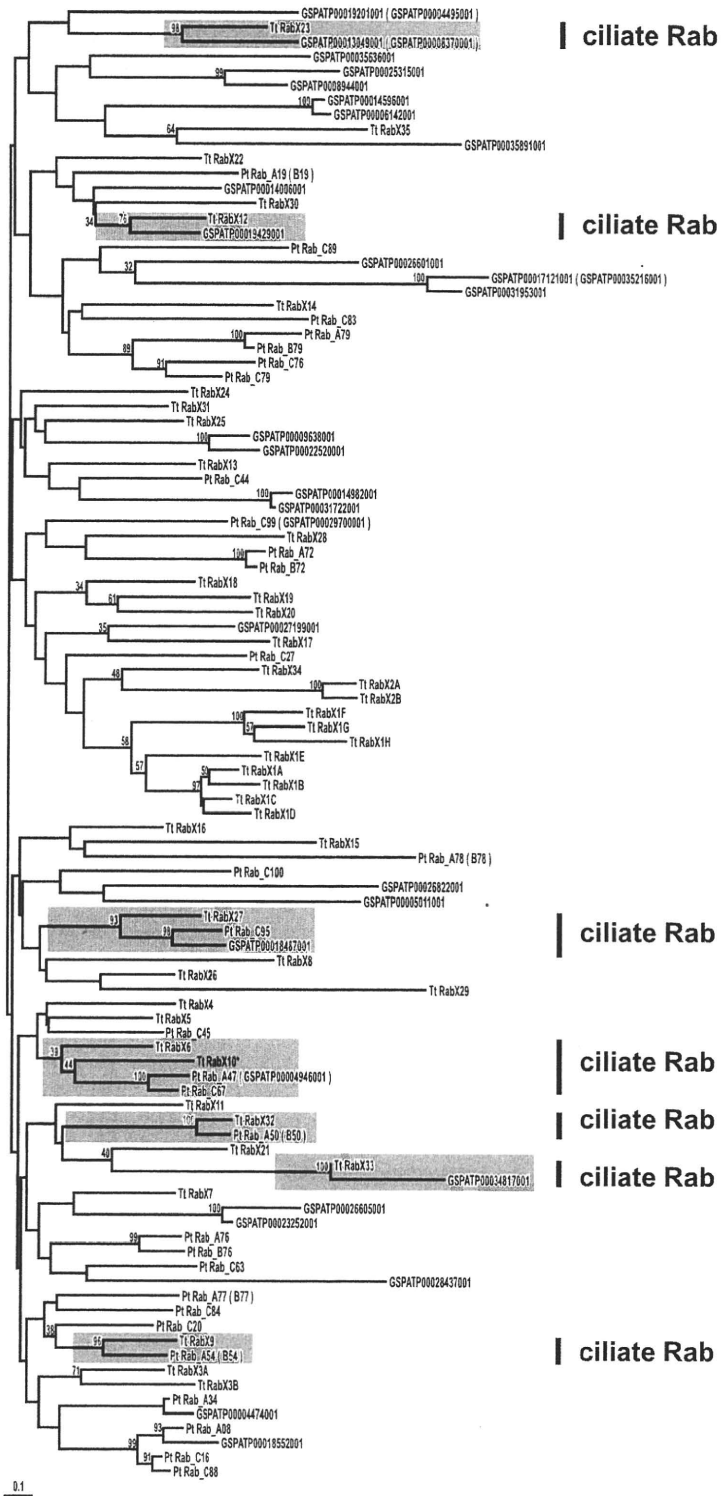

Fig. 3. A phylogenetic tree of species-specific Rab proteins from *Tetrahymena thermophila* and *Paramecium tetraurelia*. Bootstrap proportions >30% are shown. *Pt*Rab isotypes arising from genome duplication are shown in parentheses. Ciliate-specific subfamilies are highlighted by light boxes. Scale bar indicates 0.1 substitutions at each amino acid position.

Rab were considered to be present in the last eukaryotic common ancestor, because homologs Rab subfamilies are present in Opisthokonta (i.e. *H. sapiens, S. cereviviae*), Amoebozoa (i.e. *Entamoeba histolytica, Dictyostelium discoideum*), Archaeplastida (i.e. *Arabidopsis thaliana*), and Excavata (i.e. *Trypanosoma brucei, Giardia lamblia*) (Ackers, Dhir, and Field 2005; Berriman et al. 2005; Saito-Nakano et al. 2005; Vernoud et al. 2003; Weeks, Gaudet, and Insall 2005). Among the conventional *Tt*Rab, the number of constituents of *Tt*Rab1, *Tt*Rab2/4, *Tt*Rab8, *Tt*Rab11 isotypes was especially large compared with other organisms (see Table S19). Perhaps development of the secretory pathway, accompanied by increased cell volume, required an increase the number of *Tt*Rab1 and *Tt*Rab8 isotypes. In addition, human Rab1, Rab4, and Rab11 were identified on the phagosomal membrane, having roles in recycling between the phagosomal membrane and the trans-Golgi network (Garin et al. 2001). Thus, the inherent ability of phagocytosis in *T. thermophila* might be supported by the complexities of *Tt*Rab4 and *Tt*Rab11 isotypes. Coincidently, a more striking tendency toward the amplification of conventional Rab is seen in *P. tetraurelia* (Table S19), the cell volume and phagosomes of which are greater than those of *Tetrahymena*.

Diversification of species-specific Rab in ciliates. In humans, more than half of the Rab are regarded as species- or multicellular-specific Rab (Pereira-Leal and Seabra 2001); however, their expression profiles are tissue-specific, and not all *Hs*Rab are simultaneously expressed in single cells (Stenmark 2009). Thus, the observation that almost all species-specific Rab were expressed within a single cell in *T. thermophila* suggests that the multiplicity of species-specific Rab genes might perform quite different roles than Rab in other organisms.

Diversification of the Rab repertoire was also observed in *P. tetraurelia* (Table S10). Noticeable diversification of species-specific Rab was observed in amoebae, such as *E. histolytica* and *D. discoideum* (Saito-Nakano et al. 2005; Weeks et al. 2005); however, no species-specific Rab from these two amoebae showed homology, suggesting that the amoebic trafficking system is highly divergent. On the other hand, nine species-specific *Pt*Rab out of 72 showed homology to seven *Tt*RabX. Therefore, ciliate-specific Rab may be involved in ciliate-specific vesicular transport systems, and clarification of their function will be important for understanding the evolution of Rab GTPase and the membrane traffic mechanism in ciliates.

Most species-specific Rab in *T. thermophila* were not conserved in *P. tetraurelia*, and vice versa. Currently, we have little information from which to discuss the biological advantages of the diversification of species-specific Rab in ciliates. Nevertheless, one GTP-binding consensus, Box2, which is important for the GTP-hydrolysis activity of Rab, was not completely conserved in 32% of species-specific *Tt*Rab, especially in the members of the RabX1 and RabX2 subfamilies (Olkkonen and Stenmark 1997; Zuk and Elferink 2000) (Table 1). In other organisms, deletion or mutation in the GTP-binding consensus has also been reported (Saito-Nakano et al. 2005; Wilkins et al. 2005; Young, Menetrey, and Goud 2010). One of these, *Hs*Rab6C, has lost its GTP-hydrolysis activity, and plays a role in cell cycle progression but not membrane traffic (Young et al. 2010). A GTPase cycle is generally considered to be essential for the cellular function of Rab in regulating membrane dynamics. In *Tt*Rab, the functional role of deletion or mutation in the Box2 motif has not yet been clarified; however, it is possible that these incomplete *Tt*Rab might play a different role in supporting complex intracellular traffic pathways.

In addition, *Tt*RabX30 and *Tt*RabX33 had lost effecter regions RabF1 (IGVDF) (Table 1). These species-specific Rab proteins with an abnormal structural feature are possible to exert inconceivable cellular function in *T. thermophila*, respectively.

Features of the C-terminal prenylation motif of Rab in ciliates. Rab generally possesses two cysteine residues in the C-terminus, which are modified by geranylgeranylation. In contrast, other small GTPase families, such as Rho and Ras, carry a single cysteine motif, which is modified by farnesylation (Takai et al. 2001). The C-terminal cysteine motif of *Tt*Rab was classified into single or double cysteine motifs, suggesting that the targeting mechanism to the membrane might be different, perhaps because of the diversity of intracellular traffic pathways in *Tetrahymena*. Three cysteine motifs observed in *Pt*Rab have not been identified in *Tt*Rab, suggesting a *Paramecium*-specific modification system.

While 97% of the conventional *Tt*Rab contain C-terminal cysteine residues, only 50% of species-specific *Tt*Rab possess C-terminal cysteine (Table 1). Consequently, the targeting process to the membrane of species-specific *Tt*Rab might be different from the mechanism in conventional *Tt*Rab and human Rab. The same thing may go for species-specific Rab in *P. tetraurelia*; almost half of the species-specific *Pt*Rab do not possess a C-terminus cysteine motif. Deletion of the cysteine motif is also reported in Rab from other organisms; however, they have different motifs for the completion of membrane recruitment. For example, Rab5 homolog in *A. thaliana*, *At*Ara6, possesses an N-terminal myristoyl motif but not a C-terminal prenylation motif (Ueda et al. 2001). *Hs*Rab6C, also named WTH3, carries neither C-terminal cysteine nor N-terminal myristoyl motifs; however, it localizes to centrosomes, the targeting motif of which has not yet been clarified (Young et al. 2010). Thus, much remains to be learned about the novel targeting motifs and mechanisms of Rab and this will be elucidated through functional analysis of species-specific *Tt*Rab.

LITERATURE CITED

Ackers, J. P., Dhir, V. & Field, M. C. 2005. A bioinformatic analysis of the RAB genes of *Trypanosoma brucei*. *Mol. Biochem. Parasitol.*, **141**: 89–97.

Aury, J. M., Jaillon, O., Duret, L., Noel, B., Jubin, C., Porcel, B. M., Segurens, B., Daubin, V., Anthouard, V., Aiach, N., Arnaiz, O., Billaut, A., Beisson, J., Blanc, I., Bouhouche, K., Camara, F., Duharcourt, S., Guigo, R., Gogendeau, D., Katinka, M., Keller, A. M., Kissmehl, R., Klotz, C., Koll, F., Le Mouel, A., Lepere, G., Malinsky, S., Nowacki, M., Nowak, J. K., Plattner, H., Poulain, J., Ruiz, F., Serrano, V., Zagulski, M., Dessen, P., Betermier, M., Weissenbach, J., Scarpelli, C., Schachter, V., Sperling, L., Meyer, E., Cohen, J. & Wincker, P. 2006. Global trends of whole-genome duplications revealed by the ciliate *Paramecium tetraurelia*. *Nature*, **444**:171–178.

Berriman, M., Ghedin, E., Hertz-Fowler, C., Blandin, G., Renauld, H., Bartholomeu, D. C., Lennard, N. J., Caler, E., Hamlin, N. E., Haas, B., Bohme, U., Hannick, L., Aslett, M. A., Shallom, J., Marcello, L., Hou, L., Wickstead, B., Alsmark, U. C., Arrowsmith, C., Atkin, R. J., Barron, A. J., Bringaud, F., Brooks, K., Carrington, M., Cherevach, I., Chillingworth, T. J., Churcher, C., Clark, L. N., Corton, C. H., Cronin, A., Davies, R. M., Doggett, J., Djikeng, A., Feldblyum, T., Field, M. C., Fraser, A., Goodhead, I., Hance, Z., Harper, D., Harris, B. R., Hauser, H., Hostetler, J., Ivens, A., Jagels, K., Johnson, D., Johnson, J., Jones, K., Kerhornou, A. X., Koo, H., Larke, N., Landfear, S., Larkin, C., Leech, V., Line, A., Lord, A., Macleod, A., Mooney, P. J., Moule, S., Martin, D. M., Morgan, G. W., Mungall, K., Norbertczak, H., Ormond, D., Pai, G., Peacock, C. S., Peterson, J., Quail, M. A., Rabbinowitsch, E., Rajandream, M. A., Reitter, C., Salzberg, S. L., Sanders, M., Schobel, S., Sharp, S., Simmonds, M., Simpson, A. J., Tallon, L., Turner, C. M., Tait, A., Tivey, A. R., Van Aken, S., Walker, D., Wanless, D., Wang, S., White, B., White, O., Whitehead, S., Woodward, J., Wortman, J., Adams, M. D., Embley, T. M., Gull, K., Ullu, E., Barry, J. D., Fairlamb, A. H., Opperdoes, F., Barrell, B. G., Donelson, J. E., Hall, N., Fraser, C. M., Goodhead, I., Hance, Z., Harper, D., Harris, B. R., Hauser, H., Hostetler, J., Ivens, A., Jagels, K., Johnson, D., Johnson, J., Jones, K., Kerhornou, A. X., Koo, H., Larke, N., Landfear, S., Larkin, C., Leech, V., Line, A., Lord, A., Macleod, A., Mooney, P. J., Moule, S., Martin, D. M., Morgan, G. W., Mungall, K., Norbertczak, H.,

Ormond, D., Pai, G., Peacock, C. S., Peterson, J., Quail, M. A., Rabbinowitsch, E., Rajandream, M. A., Reitter, C., Salzberg, S. L., Sanders, M., Schobel, S., Sharp, S., Simmonds, M., Simpson, A. J., Tallon, L., Turner, C. M., Tait, A., Tivey, A. R., Van Aken, S., Walker, D., Wanless, D., Wang, S., White, B., White, O., Whitehead, S., Woodward, J., Wortman, J., Adams, M. D., Embley, T. M., Gull, K., Ullu, E., Barry, J. D., Fairlamb, A. H., Opperdoes, F., Barrell, B. G., Donelson, J. E., Hall, N., Fraser, C. M., Melville, S. E. & El-Sayed, N. M. 2005. The genome of the African trypanosome *Trypanosoma brucei*. *Science*, **309**: 416–422.

Bucci, C., Thomsen, P., Nicoziani, P., McCarthy, J. & van Deurs, B. 2000. Rab7: a key to lysosome biogenesis. *Mol. Biol. Cell*, **11**:467–480.

Bucci, C., Parton, R. G., Mather, I. H., Stunnenberg, H., Simons, K., Hoflack, B. & Zerial, M. 1992. The small GTPase rab5 functions as a regulatory factor in the early endocytic pathway. *Cell*, **70**:715–728.

Eisen, J. A., Coyne, R. S., Wu, M., Wu, D., Thiagarajan, M., Wortman, J. R., Badger, J. H., Ren, Q., Amedeo, P., Jones, K. M., Tallon, L. J., Delcher, A. L., Salzberg, S. L., Silva, J. C., Haas, B. J., Majoros, W. H., Farzad, M., Carlton, J. M., Smith, R. K. **Jr.**, Garg, J., Pearlman, R. E., Karrer, K. M., Sun, L., Manning, G., Elde, N. C., Turkewitz, A. P., Asai, D. J., Wilkes, D. E., Wang, Y., Cai, H., Collins, K., Stewart, B. A., Lee, S. R., Wilamowska, K., Weinberg, Z., Ruzzo, W. L., Wloga, D., Gaertig, J., Frankel, J., Tsao, C. C., Gorovsky, M. A., Keeling, P. J., Waller, R. F., Patron, N. J., Cherry, J. M., Stover, N. A., Krieger, C. J., del Toro, C., Ryder, H. F., Williamson, S. C., Barbeau, R. A., Hamilton, E. P. & Orias, E. 2006. Macronuclear genome sequence of the ciliate *Tetrahymena thermophila*, a model eukaryote. *PLoS Biol.*, **4**:e286.

Feng, Y., Press, B. & Wandinger-Ness, A. 1995. Rab 7: an important regulator of late endocytic membrane traffic. *J. Cell Biol.*, **131**:1435–1452.

Garin, J., Diez, R., Kieffer, S., Dermine, J. F., Duclos, S., Gagnon, E., Sadoul, R., Rondeau, C. & Desjardins, M. 2001. The phagosome proteome: insight into phagosome functions. *J. Cell Biol.*, **152**:165–180.

Guo, W., Roth, D., Walch-Solimena, C. & Novick, P. 1999. The exocyst is an effector for Sec4p, targeting secretory vesicles to sites of exocytosis. *EMBO J.*, **18**:1071–1080.

Horazdovsky, B. F., Busch, G. R. & Emr, S. D. 1994. VPS21 encodes a rab5-like GTP binding protein that is required for the sorting of yeast vacuolar proteins. *EMBO J.*, **13**:1297–1309.

Huber, L. A., Pimplikar, S., Parton, R. G., Virta, H., Zerial, M. & Simons, K. 1993. Rab8, a small GTPase involved in vesicular traffic between the TGN and the basolateral plasma membrane. *J. Cell Biol.*, **123**:35–45.

Jedd, G., Mulholland, J. & Segev, N. 1997. Two new Ypt GTPases are required for exit from the yeast trans-Golgi compartment. *J. Cell Biol.*, **137**:563–580.

Martinez, O., Schmidt, A., Salamero, J., Hoflack, B., Roa, M. & Goud, B. 1994. The small GTP-binding protein rab6 functions in intra-Golgi transport. *J. Cell Biol.*, **127**:1575–1588.

Miao, W., Xiong, J., Bowen, J., Wang, W., Liu, Y., Braguinets, O., Grigull, J., Pearlman, R. E., Orias, E. & Gorovsky, M. A. 2009. Microarray analysis of gene expression during the *Tetrahymena thermophila* life cycle. *PLoS ONE*, **4**:e4429.

Nilsson, J. 1979. Phagotrophy in *Tetrahymena*. *In*: Levandowsky, M. & Huter, S. H. (ed.), Biochemistry and Physiology of Protozoa. Academic Press, New York. p. 339–379.

Novick, P. & Zerial, M. 1997. The diversity of Rab proteins in vesicle transport. *Curr. Opin. Cell Biol.*, **9**:496–504.

Nuoffer, C., Davidson, H., Matteson, J., Meinkoth, J. & Balch, W. 1994. A GDP-bound of rab1 inhibits protein export from the endoplasmic reticulum and transport between Golgi compartments. *J. Cell Biol.*, **125**:225–237.

Olkkonen, V. M. & Stenmark, H. 1997. Role of Rab GTPases in membrane traffic. *Int. Rev. Cytol.*, **176**:1–85.

Paulin, J. J. 1996. Morphology and cytology of ciliates. *In*: Hausmann, K. & Bradbury, P. C. (ed.), Ciliates. Verlag Chemie Int. Inc., New York. p. 1–40.

Pereira-Leal, J. B. & Seabra, M. C. 2000. The mammalian Rab family of small GTPases: definition of family and subfamily sequence motifs suggests a mechanism for functional specificity in the Ras superfamily. *J. Mol. Biol.*, **301**:1077–1087.

Pereira-Leal, J. B. & Seabra, M. C. 2001. Evolution of the Rab family of small GTP-binding proteins. *J. Mol. Biol.*, **313**:889–901.

Robibaro, B., Stedman, T. T., Coppens, I., Ngo, H. M., Pypaert, M., Bivona, T., Nam, H. W. & Joiner, K. A. 2002. *Toxoplasma gondii* Rab5 enhances cholesterol acquisition from host cells. *Cell. Microbiol.*, **4**:139–152.

Saito-Nakano, Y., Loftus, B. J., Hall, N. & Nozaki, T. 2005. The diversity of Rab GTPases in *Entamoeba histolytica*. *Exp. Parasitol.*, **110**:244–252.

Seabra, M. C., Mules, E. H. & Hume, A. N. 2002. Rab GTPases, intracellular traffic and disease. *Trends Mol. Med.*, **8**:23–30.

Singer-Kruger, B., Stenmark, H. & Zerial, M. 1995. Yeast Ypt51p and mammalian Rab5: counterparts with similar function in the early endocytic pathway. *J. Cell Sci.*, **108**:3509–3521.

Stenmark, H. 2009. Rab GTPases as coordinators of vesicle traffic. *Nat. Rev. Mol. Cell Biol.*, **10**:513–525.

Stenmark, H. & Olkkonen, V. M. 2001. The Rab GTPase family. *Genome Biol.*, **2**, Review S3007.

Swofford, D. L., Waddell, P. J., Huelsenbeck, J. P., Foster, P. G., Lewis, P. O. & Rogers, J. S. 2001. Bias in phylogenetic estimation and its relevance to the choice between parsimony and likelihood methods. *Syst. Biol.*, **50**:525–539.

Takai, Y., Sasaki, T. & Matozaki, T. 2001. Small GTP-binding proteins. *Physiol. Rev.*, **81**:153–208.

Thompson, J., Higgins, D. & Gibson, T. 1994. CLUSTAL W: improving the sensitivity of progressive multiple sequence alignment through sequence weighting, position-specific gap penalties and weight matrix choice. *Nucleic Acids Res.*, **22**:4673–4680.

Tisdale, E. J. 1999. A Rab2 mutant with impaired GTPase activity stimulates vesicle formation from pre-Golgi intermediates. *Mol. Biol. Cell*, **10**:1837–1849.

Ueda, T., Yamaguchi, M., Uchimiya, H. & Nakano, A. 2001. Ara6, a plant-unique novel type Rab GTPase, functions in the endocytic pathway of *Arabidopsis thaliana*. *EMBO J.*, **20**:4730–4741.

Ullrich, O., Reinsch, S., Urbe, S., Zerial, M. & Parton, R. G. 1996. Rab11 regulates recycling through the pericentriolar recycling endosome. *J. Cell Biol.*, **135**:913–924.

van der Sluijs, P., Hull, M., Webster, P., Mâle, P., Goud, B. & Mellman, I. 1992. The small GTP-binding protein rab4 controls an early sorting event on the endocytic pathway. *Cell*, **70**:729–740.

Vernoud, V., Horton, A. C., Yang, Z. & Nielsen, E. 2003. Analysis of the small GTPase gene superfamily of *Arabidopsis*. *Plant Physiol.*, **131**:1191–1208.

Wang, X., Kumar, R., Navarre, J., Casanova, J. E. & Goldenring, J. R. 2000. Regulation of vesicle trafficking in madin-darby canine kidney cells by Rab11a and Rab25. *J. Biol. Chem.*, **275**:29138–29146.

Weeks, G., Gaudet, P. & Insall, R. 2005. The small GTPase superfamily. *In*: Loomis, W. & Kuspa, A. (ed.), Dictyostelium Genomics. Horizon Bioscience, Norforlk, UK. p. 173–210.

White, J., Johannes, L., Mallard, F., Girod, A., Grill, S., Reinsch, S., Keller, P., Tzschaschel, B., Echard, A., Goud, B. & Stelzer, E. 1999. Rab6 coordinates a novel Golgi to ER retrograde transport pathway in live cells. *J. Cell Biol.*, **147**:743–760.

Wilkins, A., Szafranski, K., Fraser, D. J., Bakthavatsalam, D., Muller, R., Fisher, P. R., Glockner, G., Eichinger, L., Noegel, A. A. & Insall, R. H. 2005. The *Dictyostelium* genome encodes numerous RasGEFs with multiple biological roles. *Genome Biol.*, **6**:R68.

Wilson, C., Kreychman, J. & Gerstein, M. 2000. Assessing annotation transfer for genomics: quantifying the relations between protein sequence, structure and function through traditional and probabilistic scores. *J. Mol. Biol.*, **297**:233–249.

Young, J., Menetrey, J. & Goud, B. 2010. RAB6C Is a Retrogene that Encodes a Centrosomal Protein Involved in Cell Cycle Progression? *J. Mol. Biol.*, **397**:69–88.

Zerial, M. & McBride, H. 2001. Rab proteins as membrane organizers. *Nat. Rev. Mol. Cell Biol.*, **2**:107–117.

Zuk, P. A. & Elferink, L. A. 2000. Rab15 differentially regulates early endocytic trafficking. *J. Biol. Chem.*, **275**:26754–26764.

SUPPORTING INFORMATION

Additional Supporting Information may be found in the online version of this article:

Table S1. PCR primers used in this study.

Table S2. Amino acid identities among *Tt*Rab5 subfamily of *Tetrahymena thermophila*.

Table S3. Amino acid identities among *Tt*Rab7 subfamily of *Tetrahymena thermophila*.

Table S4. Amino acid identities among *Tt*Rab1 subfamily of *Tetrahymena thermophila*.

Table S5. Amino acid identities among *Tt*Rab8 subfamily of *Tetrahymena thermophila*.

Table S6. Amino acid identities among *Tt*Rab2 and *Tt*Rab4 subfamilies of *Tetrahymena thermophila*.

Table S7. Amino acid identities among *Tt*Rab6 subfamily of *Tetrahymena thermophila*.

Table S8. Amino acid identities among *Tt*Rab11 subfamily of *Tetrahymena thermophila*.

Table S9. Amino acid identities among *Tetrahymena*-specific RabX1 subfamily of *Tetrahymena thermophila*.

Table S10. List of small GTPases in *Paramecium tetraurelia*.

Table S11. Amino acid identities among *Pt*Rab5 subfamily in *Paramecium tetraurelia*.

Table S12. Amino acid identities among *Pt*Rab7 subfamily in *Paramecium tetraurelia*.

Table S13. Amino acid identities among *Pt*Rab1 and *Pt*Rab8 subfamilies in *Paramecium tetraurelia*.

Table S14. Amino acid identities among *Pt*Rab2 and *Pt*Rab4 subfamilies in *Paramecium tetraurelia*.

Table S15. Amino acid identities among *Pt*Rab6 subfamily in *Paramecium tetraurelia*.

Table S16. Amino acid identities among *Pt*Rab11 subfamily in *Paramecium tetraurelia*.

Table S17. Amino acid identities among *Paramecium*-specific Rab subfamily.

Table S18. Amino acid identities among ciliate-specific Rab subfamilies.

Table S19. Number of members of Rab subfamilies.

Fig. S1. Expression profile of conventional Rab obtained from *Tetrahymena* Gene expression Database. For growing cells, L-l, L-m and L-h correspond respectively to 1×10^5, 3.5×10^5, and 1×10^6 cells/ml, respectively (Miao et al., 2009). For starvation, 2×10^5 cells/ml were collected at 0, 3, 6, 9, 12, 15 and 24 h (referred to as S-0, S-3, S-6, S-9, S-12, S-15 and S-24). After the conjugation, cells were collected at 0, 2, 4, 6, 8, 10, 12, 14, 16 and 18 h (referred to as C-0, C-2, C-4, C-6, C-8, C-10, C-12, C-14, C-16 and C-18). (**A**) *Tt*Rab1A subfamily, (**B**) *Tt*Rab2 and *Tt*Rab4 subfamilies, (**C**) *Tt*Rab8 subfamily, (**D**) *Tt*Rab11 subfamily, (E) *Tt*Rab5 and *Tt*Rab21 subfamilies, and (**F**) *Tt*Rab6 and *Tt*Rab7 subfamilies.

Fig. S2. Expression of profile of species-specific Rab obtained from *Tetrahymena* Gene Expression Database. Expression stage was described in Fig. S2. (**A**) *Tt*RabX1 and *Tt*RabX2 subfamilies. *Tt*RabX1A and *Tt*Rab1E are possessed the same gene ID and expression profiles. (**B**) *Tt*RabX3 subfamily and *Tt*RabX4-*Tt*RabX10. (**C**) *Tt*RabX11-*Tt*RabX20. (**D**) *Tt*RabX21-*Tt*RabX27. (**E**) *Tt*RabX28-*Tt*RabX35. Expression data of *Tt*RabX34 was not registered in TGED. (**F**) Two *Tt*Rab genes which we failed cDNA cloning.

Please note: Wiley-Blackwell are not responsible for the content or functionality of any supporting materials supplied by the authors. Any queries (other than missing material) should be directed to the corresponding author for the article.

Received: 04/23/10, 06/24/10; accepted: 06/28/10

研究論文紹介

赤痢アメーバ原虫に対するトリフルオロメチオニン誘導体の有効性*

[1] 慶應義塾大学　先端生命科学研究所，[2] 国立感染症研究所　寄生動物部

佐藤　暖[1]，野崎　智義[2]

Vitamins (Japan), **84** (5・6), 250-254 (2010)

Cytotoxic effect of amide derivatives of trifluoromethionine against the enteric protozoan parasite *Entamoeba histolytica*

Dan Sato[1], Seiki Kobayashi[2], Hiroyuki Yasui[3], Norio Shibata[3], Takeshi Toru[3], Masaichi Yamamoto[4], Gensuke Tokoro[4] Vahab Ali[5], Tomoyoshi Soga[1], Tsutomu Takeuchi[2], Makoto Suematsu[6], Tomoyoshi Nozaki[5,7]

[1]Institute for Advanced Biosciences, Keio University, Tsuruoka, Yamagata 997-0052, Japan
[2]Department of Parasitology, School of Medicine, Keio University, Shinjuku, Tokyo 160-8582, Japan
[3]Department of Frontier Materials, Graduate School of Engineering, Nagare College, Nagoya Institute of Technology, Nagoya 466-8555, Japan
[4]aRigen Pharmaceuticals Incorporated, 7-3-37/3F, Akasaka, Minato-ku, Tokyo 107-0052, Japan
[5]Department of Parasitology, Gunma University Graduate School of Medicine, Maebashi, Gunma, Japan
[6]Department of Biochemistry and Integrative Medical Biology, School of Medicine, Keio University, Shinjuku, Tokyo 160-8582, Japan
[7]Department of Parasitology, National Institute of Infectious Diseases, Shinjuku, Tokyo 162-8640, Japan

[*International Journal of Antimicrobial Agents* **35** (1), 56–61 (2010)]
[*International Journal of Antimicrobial Agents* **35** (4), 417 (2010)]

Neglected Diseases という言葉をご存じだろうか．治療を必要とする患者が多数存在するにもかかわらず，それがアジア・ラテンアメリカ・アフリカの貧しい地域に集中しているため，研究や薬剤開発が進まない病気のことである[1]．新薬の開発には通常 10 年以上の年月と数十億円以上の費用がかかるが，製薬会社がこの負担に耐えて新薬を開発したとしても，患者が貧しい人ばかりであれば収益を上げるどころか投資を回収することすらおぼつかない．したがって製薬会社はこのような薬剤開発に対して消極的になり，結果として患者は見捨てられていく．日本語では“顧みられない”病気と訳されることが多いが“Neglected”のほうが実態をより的確に表している．

先進国ではそれほどでもないが，発展途上国では大きな脅威となっている感染症は数多く存在する．赤痢アメーバ症もその一つである．赤痢アメーバ症は寄生性原虫 *Entamoeba histolytica* の感染によって起こり，途上国を中心に年間 5000 万人の患者と 7 万人の死者を出すと推定され，5 歳以下の子供の主要な死因の一つに挙げられる[2]．日本国内においても海外渡航者のほか知的障害者や男性同性愛者で蔓延が報告され，厚生労働省への届出数は 2001 年の 400 件から 2008 年の 800 件へと増加傾向にある[3]．

赤痢アメーバ原虫は不衛生な飲料水などから経口感染し，腸管内で繁殖して下痢症を引き起こす．感染した原

* 本論文は日本ビタミン学会第 61 回大会（平成 21.5.30-31 亀岡市）における発表内容について座長推薦，編集委員会寄稿依頼により講演内容をまとめたものである．

本論文の別刷請求先：〒 997-0052　山形県鶴岡市覚岸寺字水上 246-2　慶應義塾大学　先端生命科学研究所　佐藤　暖
e-mail address: dsato@z7.keio.jp

虫の一部は腸から門脈に侵入し，肝臓・肺・脳に移行して膿瘍を形成する[4]．治療には抗原虫・抗菌薬であるメトロニダゾールが使われるが[4,5]，組織や臓器に侵入した原虫にしか効果がなく，腸管に寄生した原虫への効果は低い．メトロニダゾール耐性株は現在のところ報告されていないが，薬剤が効きにくいケースは報告されており[6]，*in vitro* 培養下では簡単に作出できる．さらにアメーバと同様メトロニダゾールを治療薬とする他の病原体(嫌気性細菌や膣トリコモナス原虫)では耐性株が臨床上問題となっている[6]ことから，赤痢アメーバ原虫でも近い将来メトロニダゾール耐性株が現れることは容易に想像できる．したがって新規な作用機序をもった薬剤が求められている．

寄生虫に限ったことではないが，感染症に対する薬剤開発を考えるとき，病原体にのみ存在する代謝経路は理想的な標的となり得る．生理学的研究や全ゲノム情報，メタボロミクス研究から，赤痢アメーバ原虫にもそのような"魅力的"な代謝経路がいくつか存在することが分かってきた．その中でも含硫アミノ酸の代謝系は，ヒトには無いユニークな特徴をもつ．ヒトの体内では，食物から取ったメチオニンはシスタチオニンを経由してシステインへ代謝される．しかし赤痢アメーバ原虫にはこの経路に関する酵素活性及び遺伝子が存在せず[7]，代謝産物中にもシスタチオニンは検出されない(佐藤，未発表データ)．また，メチオニンサイクルに関与する酵素も一部欠けており，サイクルとしては途絶している[7]．一方で，本原虫は含硫アミノ酸をアンモニア・α-ケト酸・揮発性チオールに分解して代謝している．この反応はメチオニンγ-リアーゼ(Methionine γ-lyase; MGL)によって触媒される[8]．MGLは寄生性原生動物と嫌気性細菌の一部，植物で知られているが，ほ乳類には存在しない．

私たちはメチオニンのアナログであるトリフルオロメチオニン(Trifluoromethionine; TFM)をリード化合物として抗アメーバ薬の開発を進めている．TFMはメチオニンのメチル基の水素がフッ素に置き換わったアナログで約半世紀前に合成され[9]，歯周病菌を含む細菌や赤痢アメーバ原虫，トリコモナス原虫に対して *in vitro* 培養系や動物感染モデルで有効であることが報告されている[8,10,11]．私たちはTFMを上回る薬剤を開発するため，TFMの誘導体を合成して薬効を検討し，誘導体化の構造機能相関や作用機序を明らかにすることを試みた．

今までの研究から，TFMはプロドラッグ(代謝を受けた後で薬として作用する)であると考えられる．TFMは，メチオニンと構造が似ているにもかかわらずタンパク質の構成要素やメチル化反応の基質になりにくい[12,13]が，MGLによる分解は受けやすい[14]．TFMはMGLを持つ生物に取り込まれると，アンモニアとα-ケト酸のほかにトリフルオロメタンチオール(Trifluoromethanethiol; CF3SH)に分解される．CF_3SHはタンパク質を非特異的に架橋して毒性を示すと予想され[15]，実際にTFMとMGLの組み換えタンパクと反応させると架橋反応が起こる[14]．また，TFM耐性の赤痢アメーバ株ではMGL遺伝子の発現が大幅に抑制される(未発表データ)こともTFMがMGLの存在下で毒性を発揮することを暗示している．この作用機序をふまえ私たちはTFMの誘導体化に当たって以下の2点は必須であると考えた．

1. MGLと基質の反応過程では基質のα-アミノ基がPLP(MGLが持つ補酵素)と結合することが分かっている．TFM誘導体でも同様の反応が起こるためには，このα-アミノ基は保存される必要がある．
2. 毒性を示すのはCF_3SHであるので，化合物中の「CF_3S-」の構造も維持されるべきである．

私たちは残りのカルボキシル基に着目し，そこにアミド基を介して様々な官能基を導入した誘導体を15種類合成して殺アメーバ作用を検証した．

まず *in vitro* 培養下での毒性を調べた(表1)．TFMのIC_{50}は7.34 μMだったのに対してアニリド·ベンズアミド·ジフルオロアニリド誘導体では，IC_{50}が1/3.3から1/2.5に低下した(2.22-2.97 μM．TFM-01から05)．さらにメトキシアニリド誘導体では1/6に低下した(1.11-1.28 μM．TFM-07から09)．この値はメトロニダゾールのIC_{50}(4.76 μM)よりも低い．比較のためTFM-01・02・09のほ乳類由来の培養細胞(チャイニーズハムスター卵巣細胞を使用した)に対するIC_{50}を調べたところ，原虫の場合よりも100倍以上高かった．したがってこれらのアミド誘導体は有望な薬剤になると期待される．特にメトキシアニリド誘導体はジフルオロアニリド誘導体よりもフッ素(原料として高価である)が少ないので，安価に製造することが可能である．本症の患者は途上国に多いので薬剤の価格は極めて重要な点である．一方で，同じハロゲンでも塩素·臭素付加や大きな置換基(8-アミノキノリンや5,6,7,8,-テトラヒドロ-1-ナフタレンアミン)の導入ではIC_{50}がTFMより高くなることが判明した(TFM-10から15)．

誘導体化で薬効が向上した理由として，まず私たちは，これら誘導体の作用機序がTFMと根本的に異なる(すなわち薬効とCF_3-基の遊離は無関係である)と予想した．そこで，優れた薬効を示した誘導体2種類(TFM-01と09)を例に，フッ素を水素に置き換えた化合物(MET-01と09)や，CF_3SHとアンモニアが外れた後の化合物(2-oxobutananilde と 2-oxo-3',4',5'-trimethoxybutananilide; OB-01と09)を合成して殺アメーバ作用を検討した．しかしどれも薬効が全く認められなかった．この結果からアミド誘導体が薬効を示すためにはリード化合物と同様にCF_3SHの遊離が必要であると推察された．次に，誘導体化によってMGLによる分解を受けやすくなったため殺アメーバ作用が高まったと考え，アミド誘導体と組み換えMGLタンパク質と反応させて分解産物を定量した．ところが予想に反してアミド誘導体はMGLの基質になりにくいか，

全くならないことが判明した(データは紹介論文参照)．この結果を素直に受け取ると"TFM アミド誘導体は MGL によって分解されにくいが，分解産物 CF_3SH のはたらきで強い殺アメーバ作用を示す"ということになる．

この矛盾を明らかにするため，誘導体の代謝過程を追跡することを試みた．本来ならば原虫に取り込まれた薬剤の動態を見るべきであるが，取り込み効率や分析装置の検出限界などを考慮して，原虫の破砕液に TFM アミド誘導体(TFM-01)を混ぜ，分解産物を質量分析計で定量して代謝過程を推測することにした．結果を見ると，反応後 15 分で TFM が検出されるがそれ以上には増えず，そのあと 2-オキソブチル酸が検出され時間と共に増えていく(図 1 (a))．一方で OB-01 は全く検出されなかった．以上のことから，TFM アミド誘導体はいったんアミド結合が加水分解されて TFM に代謝された後，MGL によって分解されて毒性を示すと推察された．このアミド誘導体は水溶液中で安定であり自発的な分解は起こらないので，アメーバの加水分解酵素によって分解されたと考えるのが妥当である．そこでプロテアーゼ阻害剤を加えて同じ実験を行ったところ，TFM の生成量は E-64 と EDTA でそれぞれ 60％と 35％減少した(未発表データ)．したがってアミド結合の分解には少なくともシステインプロテアーゼとメタロプロテアーゼが関与すると思われる．以上をまとめた TFM アミド誘導体の分解過程の予想を図 1 (b) に示した．TFM に直接(アミド結合を介さずに)官能基を付けた誘導体は毒性を示さないことも，付加された官能基が加水分解で外れて TFM に代謝され，その後 MGL の基質になる可能性を示唆している(未発表データ)．TFM アミド誘導体で殺アメーバ作用が向上した理由は不明であるが，私たちは，誘導体化により TFM が原虫に取り込まれやすくなったからではないかと推察している．

続いて TFM アミド誘導体の薬効をハムスター肝膿瘍モデルで検討した．まずハムスター肝臓にアメーバを注射

表 1. TFM 誘導体の構造，ならびに *in vitro* 培養での殺アメーバ作用

化合物名	構造	IC50 (μM) (平均値 ± S.D.)
TFM	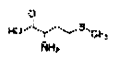	7.34 ± 0.59
TFM-01	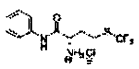	2.22* ± 0.02
TFM-02	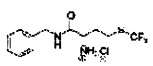	2.28* ± 0.05
TFM-03	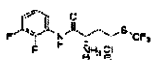	2.37* ± 0.01
TFM-04	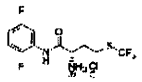	2.97* ± 0.02
TFM-05	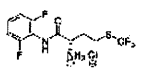	2.46* ± 0.01
TFM-06	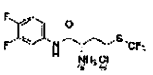	6.66* ± 0.16
TFM-07	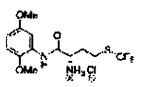	1.11* ± 0.02
TFM-08	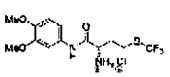	1.19* ± 0.01
TFM-09	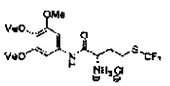	1.28* ± 0.05
TFM-10	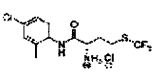	> 80

化合物名	構造	IC50 (μM) (平均値 ± S.D.)
TFM-11	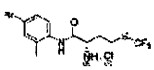	16.86* ± 0.54
TFM-12	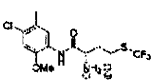	10.02 ± 0.06
TFM-13	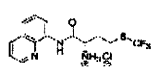	12.48 ± 0.02
TFM-14	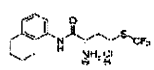	11.58 ± 0.17
TFM-15	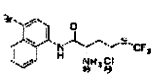	> 80
MET-01	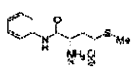	> 80
MET-09	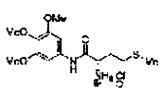	> 80
OB-01	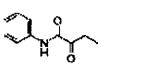	> 80
OB-09	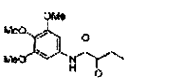	> 80
メトロニダゾール	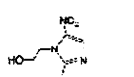	4.76* ± 0.22

*P values < 0.05 as compared to TFM

(a)

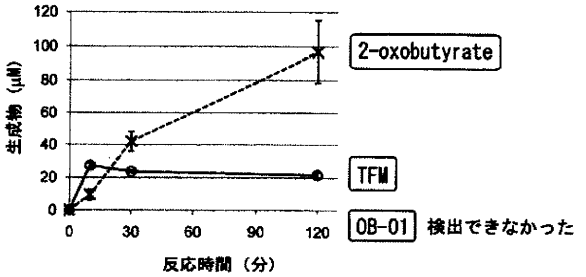

図1(a)　TFMアミド誘導体(TFM-01)の分解産物の時系列変化. 赤痢アメーバ原虫の破砕物(50 μg)とTFMアミド誘導体(2 mM)を反応させ, 分解産物をキャピラリー電気泳動 - 時間飛行型質量分析計で定量した. TFMと2-オキソブチル酸の量を示した(3回の平均値とSD). OB-01は検出されなかった

(b)

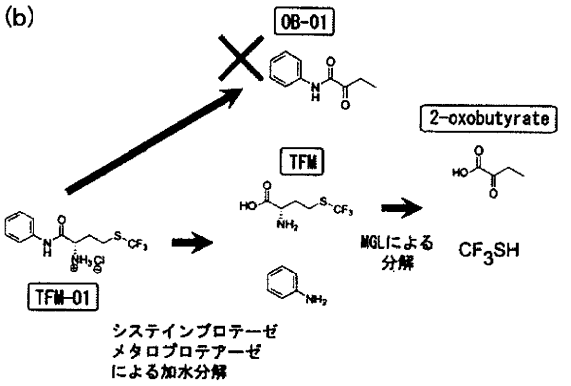

図1(b)　予想されるTFM-01の分解過程.

表2. 肝膿瘍を発症させたハムスターにTFM誘導体を腹腔投与して殺アメーバ作用を検討した結果

化合物名	day0からday6までの体重増加量(%)(平均値 ± S.E.)*	肝臓重量に対する膿瘍の割合(%)(mean ± S.E.)	動物数
TFM	22.9 ± 12.8	0.2 ± 0.2	3
TFM-01	24.5 ± 14.8	4.3 ± 4.3	2
TFM-02	13.4 ± 0.5	8.2 ± 7.9	3
TFM-03	29.1 ± 5.2	7.9 ± 7.9	3
TFM-04	41.2 ± 4.3	0.2 ± 0.1	3
TFM-05	17.9 ± 1.1	0.4 ± 0.2	3
TFM-06	26.6 ± 2.9	19.4 ± 5.6	3
TFM-07	32.6 ± 1.7	0.2 ± 0.2	2
TFM-08	27.7 ± 3.4	3.2 ± 1.5	3
TFM-09	30.3 ± 7.5	26.7 ± 13.6	3
TFM-10	25.1 ± 2.8	5.4 ± 5.2	3
TFM-11	15.4 ± 5.1	24.6 ± 6.3	3
TFM-12	45.8 ± 10.6	5.6 ± 5.6	3
TFM-13	17.7 ± 0.8	3.5 ± 0.8	3
TFM-14	30.9 ± 2.6	0.0 ± 0.0	3
TFM-15	15.3 ± 5.6	26.5 ± 9.0	3
Control**	19.1 ± 7.2	39.7 ± 1.8	3

*ハムスター肝臓にアメーバを接種し(day0), 24時間後に薬剤を腹腔投与した(day1). その5日後(day6)に肝臓を摘出した.
**DMSO(100 mL/匹).

表3. 肝膿瘍を発症させたハムスターにTFM誘導体を経口投与して殺アメーバ作用を検討した結果

化合物名	投与量	day0からday6までの体重増加量(%)(平均値 ± S.E.)*	肝臓重量に対する膿瘍の割合(%)(平均値 ± S.E.)	動物数
TFM	0.2 μmole/head (1.02 mg/kg)	35.1 ± 2.1	7.8 ± 5.9	3
	0.5 μmole/head (2.54 mg/kg)	27.6 ± 4.5	0.0 ± 0.0	3
	0.7 μmole/head (3.56 mg/kg)	34.5 ± 2.2	1.7 ± 1.4	3
	5.08 mg/kg (1.0 μmole/head)	27.7 ± 5.9	0.0 ± 0.0	3
TFM-14	0.2 μmole/head (1.84 mg/kg)	26.3 ± 3.2	30.2 ± 1.7	3
	0.5 μmole/head (4.61 mg/kg)	23.3 ± 8.3	11.3 ± 9.2	3
	0.7 μmole/head (6.45 mg/kg)	22.4 ± 2.9	3.9 ± 2.5	3
	1.0 μmole/head (9.22 mg/kg)	33.9 ± 3.7	0.0 ± 0.0	3
Control**		5.0 ± 0.9	47.6 ± 0.0	2

*ハムスター肝臓にアメーバを接種し(day0), 24時間後に薬剤を腹腔投与した(day1). その5日後(day6)に肝臓を摘出した.
**DMSO(100ml/匹).

後，24 時間飼育して肝膿瘍を形成させた．そのあと薬剤（0.2 μmole/ 匹）を一回腹腔投与し，5 日後に解剖して肝臓と膿瘍の重量を量った（表 2）．肝臓重量に占める膿瘍の割合を見ると，ジフルオロアニリド（TFM-04 と 05），メトキシアニリド（TFM-07），5,6,7,8,-テトラヒドロ -1- ナフタレンアミン（TFM-14）の投与で TFM と同様の有効性を示した．他の化合物は TFM よりも有効性が低く *in vitro* 培養での結果とは一致しなかった．また，体重増加量を見ると TFM-04・TFM-07・TFM-14 では TFM よりも大きいことから，これらは TFM よりも副作用が低いかもしれない．

この実験では簡便さを考え腹腔投与したが，薬剤として実用化された場合，投与方法はメトロニダゾールと同様に経口投与が望ましい．そこで薬効と体重増加量が最もよかった TFM-14 について，濃度を変えて経口投与（服用回数一回）して薬効を TFM と比較した（表 3）．TFM 投与では 0.5 μmole/ 匹（2.54 mg/kg に相当）で完全に肝膿瘍が治癒したのに比べ，TFM-14 の薬効は同等か若干劣る．しかしメトロニダゾールで同様の実験を行った報告[16]では，肝膿瘍の治癒に TFM の 10 倍以上高い投与量（30 μmole/ 匹，100 mg/kg に相当）を必要とすることから，私たちは TFM アミド誘導体でも十分見込みがあると考えている．

これらの TFM アミド誘導体は，作用機序から考えて MGL をもつ全ての病原体に有効であると予想される．したがって赤痢アメーバ原虫のほか，膣トリコモナス原虫や歯周病菌の治療にも使える可能性が高く，本薬剤はその克服にも貢献すると期待できる．

（平成 22.1.18 受付）

文　献

1) Hotez PJ, Kamath A (2009) Neglected tropical diseases in sub-saharan Africa: review of their prevalence, distribution, and disease burden. *PLoS Negl Trop Dis* **3**, e412

2) Haque R, Huston CD, Hughes M, Houpt E, Petri WA, Jr (2003) Amebiasis. *N Engl J Med* **348**, 1565-1573

3) 国立感染症研究所　感染症情報センター アメーバ赤痢 http://idsc.nih.go.jp/disease/En-histolytica/index.html

4) Stanley SL (2003) Amoebiasis. *Lancet* **361**, 1025-1034

5) WHO/PAHO/UNESCO report. A consultation with experts on amoebiasis. Mexico City, Mexico 28-29 January, 1997. In Epidemiol. Bull 13-14

6) Ali V, Nozaki T (2007) Current therapeutics, their problems, and sulfur-containing-amino-acid metabolism as a novel target against infections by "amitochondriate" protozoan parasites. *Clin Microbiol Rev* **20**, 164-187

7) Nozaki T, Ali V, Tokoro M (2005) Sulfur-containing amino acid metabolism in parasitic protozoa. *Adv Parasitol* **60**, 1-99

8) Tokoro M, Asai T, Kobayashi S, Takeuchi T, Nozaki T (2003) Identification and characterization of two isoenzymes of methionine gamma-lyase from Entamoeba histolytica: a key enzyme of sulfur-amino acid degradation in an anaerobic parasitic protist that lacks forward and reverse trans-sulfuration pathways. *J Biol Chem* **278**, 42717-42727

9) Dannley RL, Taborsky RG (1957) Synthesis of DL-S-trifluoromethylhomocysteine (trifluoromethylmethionine). *J Org Chem* **22**, 1275-1276

10) Yoshimura M, Nakano Y, Koga T (2002) L-Methionine-gamma-lyase, as a target to inhibit malodorous bacterial growth by trifluoromethionine. *Biochem Biophys Res Commun* **292**, 964-968

11) Coombs GH, Mottram JC (2001) Trifluoromethionine, a prodrug designed against methionine gamma-lyase-containing pathogens, has efficacy *in vitro* and *in vivo* against Trichomonas vaginalis. *Antimicrob Agents Chemother* **45**, 1743-1745

12) Duewel H, Daub E, Robinson V, Honek JF (1997) Incorporation of trifluoromethionine into a phage lysozyme: implications and a new marker for use in protein ^{19}F NMR. *Biochemistry* **36**, 3404-3416

13) Colombani F, Cherest H, de Robichon-Szulmajster H (1975) Biochemical and regulatory effects of methionine analogues in *Saccharomyces cerevisiae*. *J Bacteriol* **122**, 375-384

14) Sato D, Yamagata W, Harada S, Nozaki T (2008) Kinetic characterization of methionine gamma-lyases from the enteric protozoan parasite Entamoeba histolytica against physiological substrates and trifluoromethionine, a promising lead compound against amoebiasis. *FEBS J* **275**, 548-560

15) Alston TA, Bright HJ (1983) Conversion of trifluoromethionine to a cross-linking agent by gamma-cystathionase. *Biochem Pharmacol* **32**, 947-950

16) Pargal A, Rao C, Bhopale KK, Pradhan KS, Masani KB, Kaul C (1993) Comparative pharmacokinetics and amoebicidal activity of metronidazole and satranidazole in the golden hamster, Mesocricetus auratus. *J Antimicrob Chemother* **32**, 483-489

EUKARYOTIC CELL, June 2010, p. 926–933
1535-9778/10/$12.00 doi:10.1128/EC.00011-10

Vol. 9, No. 6

Localization and Targeting of an Unusual Pyridine Nucleotide Transhydrogenase in *Entamoeba histolytica*▽

Mohammad Abu Yousuf,[1,2] Fumika Mi-ichi,[1] Kumiko Nakada-Tsukui,[1] and Tomoyoshi Nozaki[1]*

Department of Parasitology, National Institute of Infectious Diseases, Tokyo 162-8640, Japan,[1] and Department of Parasitology, Gunma University Graduate School of Medicine, 3-39-22 Showa-machi, Maebashi 371-8511, Japan[2]

Received 17 January 2010/Accepted 3 April 2010

Pyridine nucleotide transhydrogenase (PNT) catalyzes the direct transfer of a hydride-ion equivalent between NAD(H) and NADP(H) in bacteria and the mitochondria of eukaryotes. PNT was previously postulated to be localized to the highly divergent mitochondrion-related organelle, the mitosome, in the anaerobic/microaerophilic protozoan parasite *Entamoeba histolytica* based on the potential mitochondrion-targeting signal. However, our previous proteomic study of isolated phagosomes suggested that PNT is localized to organelles other than mitosomes. An immunofluorescence assay using anti-*E. histolytica* PNT (*Eh*PNT) antibody raised against the NADH-binding domain showed a distribution to the membrane of numerous vesicles/vacuoles, including lysosomes and phagosomes. The domain(s) required for the trafficking of PNT to vesicles/vacuoles was examined by using amoeba transformants expressing a series of carboxyl-terminally truncated PNTs fused with green fluorescent protein or a hemagglutinin tag. All truncated PNTs failed to reach vesicles/vacuoles and were retained in the endoplasmic reticulum. These data indicate that the putative targeting signal is not sufficient for the trafficking of PNT to the vesicular/vacuolar compartments and that full-length PNT is necessary for correct transport. PNT displayed a smear of >120 kDa on SDS-PAGE gels. PNGase F and tunicamycin treatment, chemical degradation of carbohydrates, and heat treatment of PNT suggested that the apparent aberrant mobility of PNT is likely attributable to its hydrophobic nature. PNT that is compartmentalized to the acidic compartments is unprecedented in eukaryotes and may possess a unique physiological role in *E. histolytica*.

Pyridine nucleotide transhydrogenase (PNT) participates in the bioenergetic processes of the cell. PNT generally resides on the cytoplasmic membranes of bacteria and the inner membrane of mammalian mitochondria (3, 16) and utilizes the electrochemical proton gradient across the membrane to drive NADPH formation from NADH (14, 15, 39) according to the reaction H^+out + NADH + $NADP^+ \leftrightarrow H^+$in + NAD^+ + NADPH, where "out" and "in" denote the cytosol and the matrix of the mitochondria, or the periplasmic space and the cytosol of bacteria, respectively.

PNT has been identified in several protozoan parasites, including *Entamoeba histolytica* (8, 51), *Eimeria tenella* (17, 47), *Mastigamoeba balamuthi* (11) *Plasmodium falciparum* (10), *Plasmodium yoelii* (6), and *Plasmodium berghei* (12). In general, PNT contains conserved structural units consisting of three domains, the NAD(H)-binding domain (domain I [dI]) and the NADP(H)-binding domain (domain III [dIII]), both of which face the matrix side of the eukaryotic mitochondria or the cytoplasmic side in bacteria, and the hydrophobic domain (domain II [dII]), containing 11 to 13 transmembrane regions. PNT from *E. tenella* and *E. histolytica* exists as a single polypeptide in an unusual configuration consisting of dIIb-dIII-dI-dIIa, with a 38-amino-acid-long linker region between dIII and dI (48).

E. histolytica, previously considered an "amitochondriate" protist, is currently considered to possess a mitochondrion-related organelle with reduced and divergent functions, the mitosome (1, 21, 23a, 26, 42). Our recent proteomic study of isolated mitosomes identified about 20 new constituents (26), together with four proteins previously demonstrated in *E. histolytica* mitosomes: Cpn60 (8, 19, 21, 42), Cpn10 (46), mitochondrial Hsp70 (2, 44), and mitochondrion carrier family (MCF) (ADP/ATP transporter) (7). Despite the early presumption of PNT being localized in mitosomes (8), based on the amino-terminal region rich in hydroxylated (five serines and threonines) and acidic (three glutamates) amino acids, which slightly resembles known mitochondrion- and hydrogenosome-targeting sequences (8, 35), PNT was not discovered in the mitosome proteome. We also doubted this premise because PNT was one of the major proteins identified in isolated phagosomes (32, 33). Thus, the intracellular localization and trafficking of PNT remain unknown.

In this report, we showed that *E. histolytica* PNT (*Eh*PNT) is localized to various vesicles and vacuoles, including lysosomes and phagosomes, using wild-type amoebae and antiserum raised against recombinant *Eh*PNT and an *E. histolytica* line expressing *Eh*PNT with a carboxyl-terminal hemagglutinin (HA) epitope tag and anti-HA antibody. We also showed that all domains of *Eh*PNT are required for its trafficking to the acidic compartment by using amoeba transformants expressing the HA tag or green fluorescent protein (GFP) fused with a region containing various domains of *Eh*PNT.

MATERIALS AND METHODS

Cells, cultures, and reagents. Trophozoites of *E. histolytica* strain HM-1:IMSS cl6 were maintained axenically in Diamond's BI-S-33 medium (9) at 35.5°C.

* Corresponding author. Mailing address: Department of Parasitology, National Institute of Infectious Diseases, 1-23-1 Toyama, Shinjuku, Tokyo 162-8640, Japan. Phone: 81 3 5285 1111, ext. 2600. Fax: 81 3 5285 1219. E-mail: nozaki@nih.go.jp.

▽ Published ahead of print on 9 April 2010.

Chinese hamster ovary (CHO) cells were maintained in F12 medium (Invitrogen, San Diego, CA) supplied with 10% fetal calf serum (Medical Biological Laboratory International, Woburn, MA) at 37°C with 5% CO_2. *Escherichia coli* strains DH5α and BL21(DE3) were purchased from Life Technologies (Tokyo, Japan) and Novagen (Madison, WI), respectively. LysoTracker Red DND-99 and CellTracker Orange CMTMR [5-(and-6)-(((4-chloromethyl)benzoyl)amino)tetramethylrhodamine] were purchased from Molecular Probes (Eugene, OR). All other chemicals of analytical grade were purchased from Sigma-Aldrich unless otherwise stated.

Plasmid construction. Standard techniques were used for routine DNA manipulation, subcloning, and plasmid construction as previously described (38). To produce *E. coli* recombinant proteins, a coding region corresponding to dI (amino acids [aa] 565 to 960) of *Eh*PNT (*Eh*PNTdI) was amplified from an *E. histolytica* cDNA library by using a pair of appropriate primers designed on the basis of the nucleotide sequences in the GenBank database (accession number L39933) (8), with BamHI and XhoI restriction enzyme sites. The sense and antisense primers were 5′-CGA**GGATCC**GATGTTATTTATTGGTATTCCAA AAG-3′ and 5′-CGTT**CTCGAG**TCATTCTTCTTCAGTTGAAAGA-3′, respectively, where boldface type indicates the BamHI or XhoI site. The PCR products were cloned into the BamHI- and XhoI-digested vector pET47b (Novagen, Madison, WI), and the resulting plasmid was designated pHisPNTdI. To generate vectors to express either full-length or truncated forms of *Eh*PNT fused to HA in the amoeba, a protein-coding region corresponding to full-length *Eh*PNT (GenBank accession number AAC41577) (aa 1 to 1083), the 14-aa amino-terminal region encompassing the putative targeting sequence (TS)+dIIb (aa 1 to 330), TS+dIIb+dIII (aa 1 to 525), TS+dIIb+dIII+linker (aa 1 to 564), and TS+dIIb+dIII+ linker+dI (aa 1 to 960) was amplified from an *E. histolytica* cDNA library by using a pair of appropriate primers and cloned into the BglII site of pEhExHA (29). The antisense primers were 5′-CGT**GGATCC**ATGAAA CATTTTCAACATTCTG-3′, 5′-CGT**GGATCC**GAATGATCTATTCATAGCT TTACAC-3′, 5′-CGT**GGATCC**TTCTTCATTTAATTCTTCAAATCCTTTC-3′, 5′-CGT**GGATCC**ATCTTCTGCAAGAACTTTTGTTGGA-3′, and 5′-CGT**GG ATCC**TTCTTCTTCAGTTGAAAGAGT-3′, respectively, where boldface type represents the BamHI site. The sense primer described above was used for these full-length or truncated forms of *Eh*PNT to express in the amoeba. To generate a plasmid to express GFP fused to the *Eh*PNT TS, a pair of oligonucleotides corresponding to the TS were generated, self-annealed, and cloned into the BglII site of pEhExGFP. The oligonucleotides were 5′-**GATCT**ATGAGCACAAGTT CTAGTATTGAAGAAGAAGTGTTCAATTATA-3′ and 5′-**GATCT**ATAATT GAACACTTCTTCTTCAATACTAGAACTTGTGCTCATA-3′, where boldface type represents the truncated BglII site. pEhExGFP was generated by the ligation of the GFP protein-coding region of pKT-MG (29) into the BglII-XhoI site of pEhEx (31). These constructs allowed the expression of PNT with the three tandem copies of the HA tag or GFP at the carboxyl terminus. The resulting plasmids were designated pPNTFL-HA, pTS/IIb-HA, pTS/IIb/III-HA, pTS/dIIb/dIII/L-HA, pTS/IIb/III/L/I-HA, and pPNTTS-GFP. The production of the Cpn60-HA transformant was previously described (26).

Amoeba transformation. Plasmids generated as described above were introduced into amoeba trophozoites by lipofection as previously described (30). Geneticin (Invitrogen, San Diego, CA) was added at a concentration of 1 μg/ml at 24 h after transfection, and the Geneticin concentration was gradually increased for approximately 2 weeks until it reached 10 μg/ml.

Recombinant protein production. pHisPNTdI was introduced into BL21(DE3) cells. The expression of the histidine-tagged *Eh*PNTdI protein was induced with 1 mM isopropyl-β-thiogalactoside at 37°C for 3 h. After harvesting and washing three times with phosphate-buffered saline (PBS) (pH 7.4), the bacteria were lysed in B-PER reagent (Pierce, Rockford, IL) containing Complete Mini EDTA-free protease inhibitor cocktail (Roche Diagnostic, Mannheim, Germany) and mixed with 1.0 ml of a 50% slurry of Ni^{2+}-nitrilotriacetic acid (NTA) His-Bind resin. The recombinant *Eh*PNTdI-bound resin was washed in a column three times with 25 ml of buffer A (50 mM NaH_2PO_4, 300 mM NaCl [pH 8.0]) containing 20 mM imidazole. Bound proteins were eluted with buffer A containing 1 M imidazole and dialyzed against PBS.

Antibodies. Anti-*Eh*PNT antibody was raised against purified *Eh*PNTdI in rabbit commercially (Operon, Tokyo, Japan). Anti-HA 11MO mouse monoclonal antibody was purchased from Berkeley Antibody (Berkeley, CA). Anti-*Eh*Sec61 α-subunit and anti-*E. histolytica* dolicol-*P*-mannose synthase (*Eh*DPMS) antibodies were a gift from Rosana Sánchez-López (37). Anti-galactose/*N*-acetylgalactosamine inhibitable lectin (Hgl) monoclonal antibody (3F4) (23) was a gift from Barbara J. Mann and William A. Petri, Jr. Alexa Fluor 488- or 568-conjugated anti-mouse and anti-rabbit IgGs were purchased from Invitrogen. Alkaline phosphatase-conjugated goat anti-rabbit and goat anti-mouse IgGs were bought from Jackson ImmunoResearch Laboratories (Bar Harbor, ME). Anti-GFP rabbit antibody was purchased from Medical Biological Laboratory International.

Immunoprecipitation. Approximately 3×10^6 cells of *Eh*PNT-HA- and Cpn60-HA-expressing amoebae were lysed in lysis buffer (50 mM Tris-HCl [pH 7.5], 150 mM NaCl, 1% Triton X-100, and 0.5 mg/ml E-64). The soluble lysate, after centrifugation at 15,000 × *g*, was incubated with protein G-Sepharose beads (30 μl of a 50% slurry) (Amersham Biosciences, Uppsala, Sweden) premixed with anti-HA antibody (0.5 μl) or anti-HA and anti-Hgl antibodies, respectively.

Immunoblot analysis. Whole-cell lysate and immunoprecipitated samples were separated on either a 12% or 15% (wt/vol) SDS-polyacrylamide gel and subsequently electrotransferred onto nitrocellulose membranes (Hybond-C Extra; Amersham Biosciences, Little Chalfont, Bucks, United Kingdom) as described previously (41). The membranes were blocked by incubation in 5% nonfat dried milk in TBST (50 mM Tris-HCl [pH 8.0], 150 mM NaCl, and 0.05% Tween 20) for 1.5 h at room temperature. The blots were reacted with primary anti-*Eh*PNT rabbit or anti-HA mouse antibody at a dilution of 1:500 to 1:1,000. The membranes were washed with TBST and further reacted with alkaline phosphatase-conjugated anti-rabbit or anti-mouse IgG antibody (1:1,000) at room temperature for 1.5 h. After further washing with TBST, specific proteins were visualized with an alkaline phosphatase conjugate substrate kit (Bio-Rad, Hercules, CA).

Deglycosylation of PNT. The *Eh*PNT-HA-expressing transformant was cultured with 3 μg/ml of tunicamycin (Sigma, St. Louis, MO) for 24 h to inhibit asparagine-linked glycosylation according to a protocol described previously (22). For the chemical deglycosylation of *Eh*PNT, *Eh*PNT and fetuin were dried in a Speed Vac. Ice-cold trifluoromethanesulfonic acid (TFMS)-anisol (3:2, vol/vol [100 μl]) was added, and the samples were incubated for 4 h at 4°C under N_2 according to a method described previously (13). The reaction was stopped by slowly adding 200 μl ice-cold H_2O-pyridine (73:10, vol/vol) containing 0.1% SDS to the mixture. Anisol was extracted three times with 250 μl ethyl ether. Dialysis was performed against 2 mM pyridine acetate buffer. After dialysis, the samples were subjected to SDS-PAGE and silver staining. Immunoprecipitated *Eh*PNT was also digested with PNGase F (New England Biolabs, Ipswich, MA), an amidase that cleaves between the innermost *N*-acetylglucosamine and asparagine residues of asparagine-linked glycoproteins, according to the manufacturer's instructions.

Immunofluorescence assay and organelle staining. Amoeba transformant or wild-type amoebae in a logarithmic growth phase were harvested, transferred into 8-mm round wells on glass slides, and incubated for 30 min at 35°C to let trophozoites attach to the glass surface. An indirect immunofluorescence assay was performed as previously described (36). Briefly, amoebae were fixed with 3.7% paraformaldehyde in PBS for 10 min at room temperature. The cells were then permeabilized with 0.05% Triton X-100 in PBS for 5 min. The samples were reacted with anti-*Eh*PNT (1:100), anti-*Eh*Sec61 α-subunit (1:30), anti-*Eh*DPMS antibody (1:30), anti-GFP (1:1,000) rabbit antibody, anti-HA (1:1,000) mouse antibody, or preimmune rabbit serum (1:100). The samples were then reacted with Alexa Fluor 488- or 568-conjugated anti-mouse or anti-rabbit IgG (1:1,000).

For the staining of endosomes or late endosomes/lysosomes, amoebae were incubated with BI-S-33 medium containing 2 mg/ml rhodamine isothiocyanate (RITC)-dextran for 10 to 60 min (for endosomes) or LysoTracker Red DND-99 (Molecular Probes, Eugene, OR) (1:500) for 12 h (for late endosomes/lysosomes), respectively. To visualize phagosomes, CHO cells prestained with 10 μM CellTracker Orange or 20 μM CellTracker Blue were added to *E. histolytica* trophozoites in 8-mm wells on a glass slide and incubated for 10 to 60 min. The samples were examined on an LSM 510 Meta confocal laser scanning microscope (Carl Zeiss, Thornwood, NY). Images were further analyzed by using LSM510 software.

RESULTS

Identification of two isotypes of PNT in *E. histolytica*. Two isozymes of PNT have been identified in the *E. histolytica* genome database at Pathema (http://pathema.tigr.org/tigr-scripts/pathema/) (EHI_055400 and EHI_014030, corresponding to GenBank accession numbers XP_001914099 and AAC41577, respectively). They showed 90% mutual amino acid identity. The latter *Eh*PNT isotype (EH_014030) is 1,083 aa long with a predicted molecular mass of 117.0 kDa and a pI of 5.39. This predicted protein is identical to the PNT protein previously reported (GenBank accession number AAC41577)